

Review

Could Commercially Available Aqueous Binders Allow for the Fabrication of Highly Loaded Sulfur Cathodes with a Stable Cycling Performance?

Wenli Wei ¹, Marzi Barghamadi ¹, Anthony F. Hollenkamp ¹ and Peter J. Mahon ^{2,*} 

¹ CSIRO Manufacturing, Research Way, Clayton, VIC 3168, Australia; wenli.wei@csiro.au (W.W.); marzi.barghamadi@csiro.au (M.B.); tony.hollenkamp@csiro.au (A.F.H.)

² Department of Chemistry and Biotechnology, School of Science, Computing and Engineering Technologies, Swinburne University of Technology, Melbourne, VIC 3122, Australia

* Correspondence: pmahon@swin.edu.au

Abstract: In this review, the application of five commercially available aqueous-based binders including sodium carboxyl methyl cellulose (CMC), polyacrylic acid (PAA), polyvinyl alcohol (PVA), polyethylene oxide (PEO), and polyethyleneimine (PEI) as well as some representative custom (or purpose) synthesized functional binders used in lithium sulfur (Li-S) batteries is summarized based on the main evaluation criteria of cycling capacity, battery lifetime, and areal sulfur loading (and, consequently, energy density of the battery). CMC with SBR (styrene butadiene rubber) has been reported with promising results in highly loaded sulfur cathodes (>5 mg cm⁻² sulfur loading). PVA and PEI were confirmed to provide an enhanced adsorption of lithium polysulfides due to the interaction with hydroxyl and amine groups. No competitive advantage in electrochemical performance was demonstrated through the use of PAA and PEO. Water-based binders modified with polysulfide-trapping functional groups have complex fabrication processes, which hinders their commercial application. In general, achieving a high capacity and long cycling stability for highly loaded sulfur cathodes using commercial aqueous-based binders remains a significant challenge. Additionally, the scalability of these reported sulfur cathodes, in terms of complexity, cost, and stable electrochemical cycling, should be evaluated through further battery testing, particularly targeting pouch cell performance.

Keywords: lithium–sulfur batteries; aqueous-based binder; highly loaded sulfur cathode



Citation: Wei, W.; Barghamadi, M.; Hollenkamp, A.F.; Mahon, P.J. Could Commercially Available Aqueous Binders Allow for the Fabrication of Highly Loaded Sulfur Cathodes with a Stable Cycling Performance?

Batteries **2024**, *10*, 67. <https://doi.org/10.3390/batteries10020067>

Academic Editors: Yushi He and Zhong Ma

Received: 8 January 2024

Revised: 13 February 2024

Accepted: 15 February 2024

Published: 19 February 2024



Copyright: © 2024 by the authors. Licensee MDPI, Basel, Switzerland. This article is an open access article distributed under the terms and conditions of the Creative Commons Attribution (CC BY) license (<https://creativecommons.org/licenses/by/4.0/>).

1. Introduction

Since their introduction to the market in 1991, lithium ion (Li-ion) batteries have become the dominant form of energy storage in all portable electronic devices, including mobile phones, laptops, etc. [1]. The significance of this work for modern society was recognized by the Nobel Prize for Chemistry in 2019. Since the first generation of Li-ion batteries, which used LiCoO₂ as the cathode and graphite as the anode with a relatively low specific energy of ~80 Wh kg⁻¹, an enormous and ongoing research effort has been devoted to finding new electrode materials aiming towards raising specific energy. Today, Li-ion technology features a broad range of cathode materials, including LiFePO₄ (LFP), LiMn₂O₄ (LMO), LiNi_xMn_yCo_zO₂ (NMC), and LiNi_xCo_yAl_zO₂ (NCA), which are widely used in commercial batteries. While the enhancement of specific energy has been remarkable, with values in the range 200–280 Wh kg⁻¹ at the cell level [2], typical applications such as in electric vehicles are challenging researchers to reach even higher levels of energy/power output performance [3]. Targets of 350 Wh kg⁻¹ (specific energy) and 750 Wh L⁻¹ (energy density) at the cell level were proposed by the U.S. Department of Energy (DOE) and the U.S. Advanced Battery Consortium (USABC) in 2017 for automotive batteries [4]. However, the pathway to further gains in specific energy, for either cathode or anode materials, is

unclear. A factor that complicates the continued development of existing materials (e.g., metal oxide cathodes) is the growing realization that metal-based resources are likely to become increasingly limited in the near future, especially for Ni and Co [5]. A rechargeable battery technology that is free of such constraints is, therefore, highly desirable.

In response, the last two decades have seen increasing research efforts devoted to a range of new technologies, examples of which are lithium–sulfur, lithium–oxygen, sodium-ion, potassium-ion, zinc-ion and zinc–air [6]. Lithium–sulfur (Li-S) is one of the chemistries that has attracted a great deal of interest, mainly because of the use of sulfur (cathode, theoretical capacity of 1672 mAh g^{-1}) and lithium metal (anode, theoretical capacity of 3860 mAh g^{-1}), in which the former offers a significant weight saving in cell components. While the theoretical specific energy is impressively high (2600 Wh kg^{-1}), conservative estimates suggest that practical levels of specific energy around two times that of Li-ion technology should be achievable in the first commercial variants. Not surprisingly, such considerations are proving to be significant for applications in which mass is a critical factor, such as in CubeSat satellites and unmanned aerial vehicles (UAVs) [7]. Furthermore, sulfur has the attractive features of a low cost, high natural abundance, and environmental friendliness compared to many of the transition metals used in Li-ion battery cathodes. However, it should be noted that the promised performance improvements of the Li-S battery assume that the new technology will be able to conform to a configuration that is similar to that used in current Li-ion technology. Specifically, it will be necessary to produce Li-S batteries in which the loadings of electrode materials are on a par with those now being reached with Li-ion electrodes. Calculations have shown that, on a charge basis, an areal loading of $\sim 1.5 \text{ mg cm}^{-2}$ of sulfur on the cathode is required to match the capacity of a typical Li-ion cathode. This suggests that in order to realize a minimum requirement in specific energy to outperform the current state of the art of Li-ion, a target of at least 5 mg cm^{-2} sulfur must be set [8].

The practical demonstration of highly loaded sulfur cathodes is still hindered by several challenging issues. The first is that octa sulfur (S_8), as the most stable sulfur allotrope, is electronically insulating (electric conductivity of S_8 and NMC811 are 5×10^{-14} and 2.1 S.m^{-1}). This can greatly limit its utilization, as the electron flow required for charging/discharging is limited to very short distances. The solution is to deploy sulfur onto a porous, conductive ‘backbone’ which operates as a sulfur host and support. Carbon is the material of choice here, but there is ongoing research into the best combination of pore size and surface area to optimize electrode performance [9,10]. Once in service, the chosen morphology must also allow for the easy diffusion of lithium ions throughout the cathode to maintain charge neutrality. The second issue concerns the complex chemistry of sulfur redox reactions and associated interactions with lithium ions [8]. When sulfur in the cathode is reduced during discharge, a variety of species, known as polysulfides (Li_2S_n , $n = 3\text{--}8$), are formed. These polysulfides are in the form of sulfur chains with two terminal negative charges that are balanced by associated lithium ions. Successive reduction produces shorter-chain species with full capacity obtained when all sulfur is converted to Li_2S . Eventually, the reaction tail of solid-state Li_2S_2 produces insoluble and nonconductive solid Li_2S . This two-step discharge process is apparent in the voltage profile of Li-S batteries, higher and lower voltage plateaus in which the latter is induced by the transformation from the long-chain lithium polysulfides to short-chain lithium sulfides and contributes the majority of the discharge capacity, i.e., around 75% of the theoretical capacity [11].

The discharge plateaus are presented in Figure 1. As noted, full capacity is only available when all polysulfides are converted to Li_2S . In practice, however, the solubility of lithium polysulfides (in the chosen electrolyte system) allows them to move away from the cathode before undergoing complete reduction. After diffusing through the polymer separator, they reach the lithium anode where they can undergo further reaction. The lower polysulfides formed in this way can behave in the following ways: (i) diffuse back to the cathode, where they undergo further redox processes; (ii) undergo further reduction at the anode, ultimately through to Li_2S , which is incorporated into the solid electrolyte interphase (SEI). Process

(i) is commonly known as the polysulfide ‘shuttle’, as it can lead to a portion of the active material moving back and forth between the two electrodes. It is directly responsible for the self-discharge of the cell, thereby decreasing the available discharge capacity. Process (ii) is effectively irreversible, so that it constitutes the permanent loss of the cathode capacity [1,12]. There are two further factors that are limiting the commercialization of Li-S batteries. First, the large volumetric expansion that occurs in the cathode during discharge due to the difference in molar volumes of sulfur atoms ($15.53 \text{ cm}^3 \text{ mol}^{-1}$) and Li_2S ($27.68 \text{ cm}^3 \text{ mol}^{-1}$). This can seriously damage the structural integrity of the cathode, where the designed backbone structure may collapse after several cycles [8] and, for highly loaded cathodes, it is likely to become more difficult to ensure cathode integrity during the coating, drying, and cycling stages. Second, the lithium anode is subject to a number of issues, including unstable SEI, surface passivation, and uncontrolled lithium dendrite growth [13].

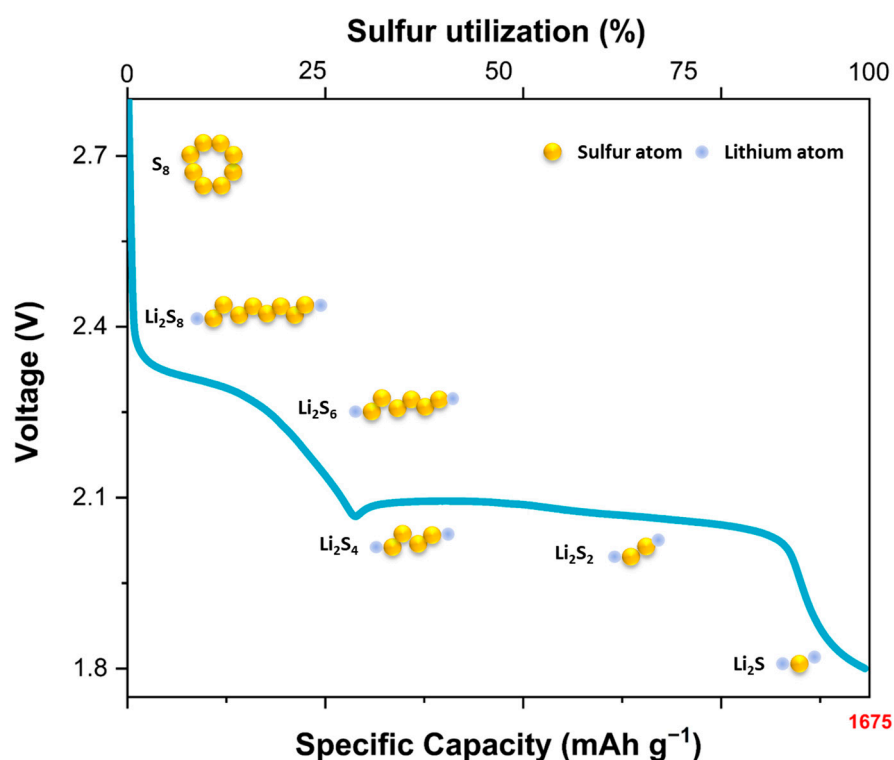


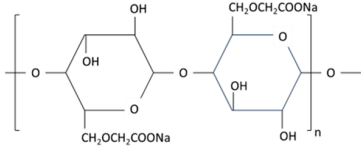
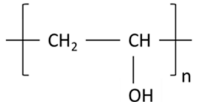
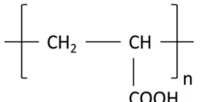
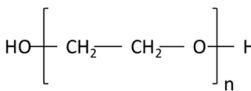
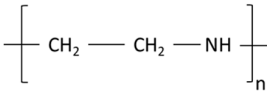
Figure 1. Typical discharge curve of Li-S batteries.

In the past decades, through extensive fundamental research, some enhancement of electrochemical performance has been achieved at a lab-scale level. Unfortunately, most of these works are based on batteries with a sulfur loading lower than 2 mg cm^{-2} , which translates to very low energy density devices. A simple scale-up from low-loading electrode configurations to fabricate highly loaded Li-S batteries is unrealistic, since the thicker layer will introduce completely new dilemmas occurring not only in electrochemical testing, but also in the fabrication and cell assembly process as discussed above. Thus, finding the appropriate roadmap to develop a high-performance sulfur cathode with a high sulfur loading is decisive in developing practical Li-S batteries. Brückner et al. [14] systematically investigated the impact of current rate, electrolyte amount, and sulfur loading for the Li-S battery cycling performance and concluded that the combination of a high rate, low loading with an excess amount of the electrolyte could lead to capacity and stability improvements but prevent achieving high energy densities. Thus, the amounts of electrolyte and areal sulfur loading are the preconditions for determining the performance of sulfur cathode materials.

As noted earlier, the use of sulfur as an electrode material requires a conductive host, similar to Li-ion battery electrodes, with a slurry formed after adding a binder mixed in a solvent that is then typically coated onto a substrate, typically a metal foil. The

binder usually accounts for a maximum of 10 wt.% of the total electrode slurry (which is a larger portion compared to Li-ion battery electrodes). The properties of the binder largely determine both the adhesion of the electrode materials to the substrate and the cohesion between the electrode material particles. The former results in a coating that does not become detached from the substrate during service, while the latter ensures the integrity of the active material mass so that no cracks develop during processing. Another factor related to binder performance is the requirement for the uniform dispersion of sulfur-infused host particles and binders, as this ensures the maximum utilization of sulfur by promoting the diffusion of ions and matching electronic conductivity throughout the cathode backbone.

Poly (vinylidene difluoride) (PVDF) is a binder that is widely used in the Li-ion battery industry and was also initially used in lithium–sulfur batteries due to its chemical stability and wide electrochemical potential window [15]. However, some of its other properties now limit its use, particularly as higher levels of performance are being sought. First, the combination of predominantly linear polymer chains and relatively weak intermolecular forces does little to oppose the intra-cathode forces that drive the structural collapse of the cathode. These properties of PVDF also provide no substantial barrier to the movement of polysulfides (Li_2S_x shuttling) [16]. There is also evidence that PVDF eventually undergoes physical degradation in ether-based electrolytes, according to reports of swelling and dissolution [17]. Furthermore, the use of PVDF requires an N-methyl-2-pyrrolidone (NMP) solvent, a substance that is toxic and also causes serious environmental problems [18]. NMP also has a relatively high boiling point where removal under heating and vacuum could potentially lead to some sulfur loss during cathode preparation. These issues inspire research into stable, environmentally friendly binders that can replace PVDF in the fabrication of highly loaded sulfur cathodes. Aqueous binders, including derivatives of natural substances such as cellulose, as well as synthetic polymers such as poly(acrylic acid) (PAA), have molecular structures and functional groups that may strengthen electrode structure and possibly aid the adsorption of lithium polysulfides. Importantly, their inherent water solubility removes the need for toxic organic solvents such as NMP, thereby aligning with the growing demand for eco-friendly battery technologies. This range of prospective benefits provides a clear justification to explore the implementation of aqueous binders in Li-S batteries. Although there are a few review papers on this topic [15,19], this is a rapidly evolving field, thereby establishing a critical need for a timely review of state-of-the-art developments. Unlike the other recent reviews, herein, we focus on highly loaded sulfur cathodes with commercially available aqueous binders, which express a more practical application and, in this context, we discuss the challenges of thick cathodes. Five of the main commercially available aqueous binders, including sodium carboxymethyl cellulose (CMC), polyacrylic acid (PAA), polyvinyl alcohol (PVA), polyethylene oxide (PEO), and polyethylenimine (PEI), are reviewed and evaluated for their applicability in the fabrication of highly loaded sulfur cathodes to realize practical Li-S batteries. A summary of the molecular structures of these binders as well as their mechanical properties is provided in Scheme 1.

Aqueous Binder	Molecular structure	Mechanical properties
Carboxymethylcellulose (CMC)		High chain stiffness High Young's modulus High viscosity, strong peeling strength Shear thinning behavior
Poly (vinyl alcohol) (PVA)		Low Young's modulus and low tensile strength
Poly (acrylic Acid) (PAA)		High adhesion strength High Young's modulus
Polyethylene Oxide (PEO)		Low modulus of elasticity and tensile strength
Polyethylenimine (PEI)		High viscosity and high tensile strength

Scheme 1. The molecular structure of five commercially available aqueous binders of CMC, PVA, PAA, PEO, and PEI and their mechanical properties.

2. Aqueous Binders

In the following sections we present a summary and interpretation for some of the previously reported research on aqueous-based binders.

2.1. Carboxymethyl Cellulose (CMC) Binders

The abundant carboxyl and hydroxyl groups in the molecular structure of carboxymethyl cellulose (CMC) make it soluble in water with an extended polymeric conformation, which is beneficial for homogeneous slurry making [19]. A number of research groups have investigated the use of CMC as a binder for sulfur cathodes (see Table 1 at the end of this section). In an early study, Kim's group [20] investigated the binder performance of several polymer binders and some combinations thereof: polyvinylpyrrolidone (PVP), polytetrafluoroethylene (PTFE), PTFE with polyvinyl alcohol (PTFE + PVA), and PTFE + CMC. They found that cathodes formulated with a PTFE + CMC binder exhibited the greatest enhancement of capacity, which they attributed to the effect of CMC in regulating the pore distribution of the cathode. Later, interest shifted to the mixed binder sodium carboxymethyl cellulose–styrene butadiene rubber (CMC + SBR), which is a widely used binder for graphite anodes of Li-ion batteries. The highly elastic nature of SBR helps compensate for the brittleness that is sometimes found in electrodes containing CMC. CMC is often used as the thickener and dispersant to prepare the homogenous electrode slurry with SBR, ensuring cohesion between sulfur and conductive additives as well as adhesion between the cathode and current collector. Compared with PVDF, the improved uniform distribution of sulfur particles and carbon black in CMC + SBR binder was confirmed by He et al. [21]. They reported that the presence of the carboxylate groups within the adsorbed layer of CMC increases effective surface charge on carbon black and, therefore, stabilizes the dispersion of carbon and sulfur particles. This enhancement of particle distribution, which is maintained as the coating dries, allows for a more efficient utilization of active sulfur and, hence, increases the cathode capacity. Both the EIS and SEM

results showed that the S/CMC + SBR cathode exhibited a more stable interface structure and electron transfer network compared with the S/PVDF cathode structure during cycling. Rao et al. also fabricated sulfur cathodes using CMC + SBR as the binder [22,23], where they pointed out that the intimate contact of sulfur with the conductive additives in conjunction with the binder elasticity dominates the cathode performance. Meanwhile, the dispersion mechanism of CMC + SBR, sodium alginate (SA), and LA132 polymer (acrylonitrile multi-copolymer) binders in sulfur cathodes was systemically studied by Rui's group [24]. They revealed that both electrostatic and stereo-chemical factors had the most impact on the quality of the cathode material slurry. The CMC chain revealed the highest charge density from Zeta potential tests and, with the help of elastic SBR, exhibited the best chain flexibility. Thus, the sulfur cathode with CMC + SBR achieved a better capacity retention during cycling, although LA132 with a high chain flexibility showed a higher initial capacity.

As summarized in Table 1, the advantages of CMC + SBR binders in Li-S batteries have been explored by several groups, but only for cathodes with low sulfur loadings and only for a limited number of cycles. In 2015, Lv et al. [25] explored the construction and challenges of highly loaded sulfur electrodes with CMC + SBR as the binder. The main concerns were focused on maintaining integrated thick coatings, without any cracking or pinholes, that were also sufficiently conductive and completely wetted by the electrolyte. They proposed the strategy of constructing a secondary interconnection between primary nanoparticles to make an integrated carbon host material. First, sulfur was infused into porous Ketjen black (KB), the carbon host. These primary nanoparticles were then covered by an amorphous carbon layer as the secondary coating. With this strategy, it was shown that a high sulfur loading of up to 8 mg cm^{-2} can be achieved. The replacement of traditional carbon additives with graphene and carbon nanotubes (CNT) resulted in a cathode with a 4.7 mg cm^{-2} sulfur loading, exhibiting a capacity of 700 mAh g^{-1} at 0.2 C after 90 cycles and a capacity retention of $\sim 70\%$ after 100 cycles. Afterwards, Lemarie et al. also explored the combination of a CMC binder with a macro porous current collector in their sulfur cathode design [26]. They adopted the operando acoustic emission to detect the degradation phenomena occurring in the sulfur electrodes during the first plateau of the initial discharge process, which indicated the initial dissolution of sulfur into the electrolyte and the reconstruction of the electrode network. Two kinds of binders (PVDF and CMC) and two current collectors (Al foil and porous carbon paper) were compared. The combination of a CMC binder and a porous carbon paper current collector was confirmed to achieve an improved performance, with an initial capacity of 1180 mAh g^{-1} at 0.02 C and a retained capacity of 860 mAh g^{-1} after 50 cycles at 0.02 C with a sulfur loading of 4 mg cm^{-2} . Meanwhile, an in situ citric acid cross-linked CMC binder (CMC-CA) was also used to achieve a high-areal-sulfur-loading cathode and a better capacity retention. The crosslinking polymerization is a result of the esterification of $-\text{OH}$ groups of CMC and $-\text{COOH}$ groups of citric acid. Nazar's group mixed N-doped graphene/graphitic C_3N_4 -sulfur powders, carbon additives, CMC, and CA together to make a slurry [27]. During this process, the CMC chains were linked by small CA molecules to form a reticular structure through a condensation reaction. With the elastomeric contact between the components in the cathode, the cathode was flat with no cracks after removal of the slurry solvent. In this way, compact, thick coatings could be prepared with sulfur loadings up to 14.9 mg cm^{-2} . However, to demonstrate the cycling capability of these cathodes, the authors employed a much thinner coating, at 2 mg cm^{-2} , for which the capacity remained at 1100 mAh g^{-1} at 0.5 C after 100 cycles. Huang et al. also selected the CMC-CA binder to optimize the lithium sulfur system [28]. They used a CMC-CA binder, Toray carbon paper current collector, and a separator coated with reduced graphene oxide. The optimized battery maintained a capacity of 960 mAh g^{-1} after 200 cycles with a sulfur loading of 2.5 mg cm^{-2} at 0.1 C . A longer cycling lifetime could be achieved for a similar sulfur loading but only at a lower current density. Compared to Nazar's work, which aimed to construct highly loaded sulfur cathodes by coupling multifunctional and hierarchical sulfur composites with an in situ cross-linked CMC-CA binder, Huang's team explored the

CMC–CA binder and optimized current collectors and separators to improve the electrochemical performance. CMC–CA may act as another reasonable choice for highly loaded sulfur cathodes along with other optimized components.

Similar to a CMC + SBR binder, carboxymethylcellulose combined with nitrile–butadiene rubber (CMC + NBR) has also been used in lithium sulfur batteries, driven by its claimed high flexibility and strong binding force [29]. A sulfur cathode with a loading of 4.5 mg cm^{-2} using the CMC + NBR binder delivered $\sim 350 \text{ mAh g}^{-1}$ at 0.2 C after 100 cycles. CMC + NBR could assist in highly loaded sulfur cathode construction but exhibited no competitive electrochemical performance advantages compared with CMC + SBR, as mentioned earlier.

Recently, Li et al. explored the electrochemical performance enhancement of a CMC binder in sulfurized polyacrylonitrile (SPAN) electrodes, with comparisons made with PVDF-bound equivalents. The authors cite the ability of CMC to capture polysulfide through the abundant oxygen functional groups present in CMC [30]. With the help of a CMC binder, the SPAN cathode could deliver a capacity of 938 mAh g^{-1} at 0.9 C after 500 cycles and maintain 677 mAh g^{-1} at a rate of 5 C but with a low sulfur loading of 1 mg cm^{-2} . Shaibani et al. [31] constructed a highly loaded sulfur cathode with only a CMC binder by adopting a strategy of lowering the solvent content per gram of electrode ingredients. They proposed to minimize the amounts of high-modulus binders between neighboring particles, which could provide more space for the material’s expansion and ion diffusion during cycling. The maximum sulfur loading for this so-called ‘expansion-tolerant’ cathode was up to 15 mg cm^{-2} . Coin cells with a sulfur loading of 6 mg cm^{-2} exhibited a capacity of around 1000 mAh g^{-1} at 0.2 C after 100 cycles. An eight-layered pouch cell with sulfur loadings of up to 12 mg cm^{-2} exhibited a discharge capacity of 1000 mAh g^{-1} at 0.1 C after 40 cycles. Afterwards, the same group [32] presented a saccharide-based binder system, and the same strategy was utilized to construct the thick sulfur cathode; glucose was further introduced in combination with the CMC binder to regulate the polysulfides due to its reducing properties. This binder system could promote the formation of viscoelastic filaments during casting, which endowed the sulfur cathode with a desirable web-like microstructure. This cathode exhibited a capacity of 700 mAh g^{-1} at 0.2 C for 1000 cycles at a 3 mg cm^{-2} sulfur loading, but no obvious capacity improvement was observed for thick cathodes deployed in coin or pouch cell configurations. Above a loading of 5 mg cm^{-2} , the performance was similar to their previous work [31].

Table 1. CMC binder in Li-S cathodes.

Binder	Cathode	Carbon Additives	Current Collector	Areal Sulfur Loading (mg cm^{-2})	Coin Cell Performance		Ref.
					Initial Capacity (mAh g^{-1})	Cycling Performance (mAh g^{-1})	
CMC + PTFE (2:18)	Sulfur	Super P	Al foil	1.05	~	~	[20]
CMC + SBR (1:1)	Sulfur	Carbon black	Al foil	~	870 (at 100 mA g^{-1})	580 (at 100 mA g^{-1} after 60 cycles)	[21]
CMC + SBR (2:3)	CNF–sulfur	Carbon black	Carbon-coated Al foil	~	1313 (at 0.05 C)	586 (at 0.05 C after 60 cycles)	[22]
CMC + SBR (2:3)	Carbon–sulfur composites	Carbon nanofibers + Carbon particles	Carbon-coated Al foil	~	1200 (at 0.05 C)	668 (at 0.05 C after 50 cycles)	[23]
CMC + SBR (1:1)	Sulfur–KB composite	Super P	Al foil	0.7–1	1046 (at 0.2 C)	821 (at 0.2 C after 50 cycles)	[24]
CMC + SBR	Sulfur/integrated KB	Graphene/MWCNT	Carbon-coated Al foil	4.7	1200 (at 0.05 C)	700 (at 0.2 C after 90 cycles)	[25]
CMC + SBR (2:1)	Sulfur/KB	KB	3D Al foam	17.7	~	~	[33]
CMC–CA (9:1)	NG–CN/S composite	CNTs/Super P	AvCarb P50 paper	2	1340 (at 0.05 C)	1100 (at 0.5 C after 100 cycles)	[27]
CMC–CA (9:1)	Sulfur/KB	MWCNT/KB	Toray carbon paper	2.5	1600 (at 0.1 C)	960 (at 0.1 C after 200 cycles)	[28]

Table 1. Cont.

Binder	Cathode	Carbon Additives	Current Collector	Areal Sulfur Loading (mg cm ⁻²)	Coin Cell Performance		Ref.
					Initial Capacity (mAh g ⁻¹)	Cycling Performance (mAh g ⁻¹)	
CMC + NBR	Sulfur	Super P	Al foil	4.6	770 (at 0.05 C)	410 (at 0.05 C after 40 cycles)	[29]
CMC	Sulfurized polyacrylonitrile	Carbon black	Al foil	1	~	938 (at 0.9 C after 450 cycles)	[30]
CMC	Sulfur	Super P	Non-woven carbon paper	4 ± 0.4	1180 (at 0.02 C)	860 (at 0.02 C after 50 cycles)	[26]
CMC	Colloidal sulfur	Carbon	Al foil	6–15	1670 (at 0.1 C)	1000 (at 0.2 C after 100 cycles) (6 mg cm ⁻²)	[31]
CMC–glucose	Sulfur	Conductive carbon powder	Al foil	2–11	1629 (at 0.2 C)	700 (at 0.2 C after 1000 cycles) (3 mg cm ⁻²)	[32]

2.2. Polyvinyl Alcohol (PVA) Binders

Polyvinyl alcohol is a linear polymer that was first used, along with PEO, as a binder in sulfur cathodes by Nakazawa's group [34]. They focused on the compatibility of a PVA binder with various levels of saponification in a solvate ionic liquid (SIL) electrolyte and found that the electrolyte uptake of the PVA binder increased on decreasing the degree of saponification, which increased the cell capacity. The polar -OH groups were considered to be active in trapping lithium polysulfides during cycling. The interaction between the -OH of PVA and various lithium polysulfides was systematically examined through theoretical DFT calculations and an experimental *ex situ* adsorption study by Liao's group [35], as shown in Figure 2a. They confirmed the enhanced lithium sulfide's trapping ability compared with PVDF. Moreover, based on DFT calculations, PVA contributed more binding energy in a thick cathode coating compared with the PVDF binder for highly loaded Li-S battery. Figure 2b clearly demonstrates that the sulfur cathode with a PVA binder, featuring high sulfur loading, exhibits a more stable and integrated structure as evidenced by optical and SEM images. However, these high-sulfur-loading cathodes with a maximum of 10.5 mg cm⁻² only maintained a low specific discharge capacity around 400 mAh g⁻¹ within 200 cycles. Chen et al. fabricated a cross-linked binder using hydrogen-bonded crosslinking between -OH groups in PVA and -COO- groups in lithium polyacrylate (LiPAA) [36]. The robust 3D cross-linking polymer binder in the sulfur cathode is shown in Figure 2c. They found that the cross-linked network maintained mechanical strength, the LiPAA with a high Li⁺ capacity ensured good ion conductivity, and the abundant polar groups in the PAA and PVA chains provided the strong anchoring ability for lithium polysulfides. The tested cathode had a low sulfur loading of 4.0 mg cm⁻² and delivered a discharge capacity of 646.9 mAh g⁻¹ after 100 cycles. The performances of these electrodes are compared in Table 2, and it is noted that none of the reported cells delivered high-capacity retention.

Table 2. PVA binder in Li-S cathodes.

Binder	Cathode	Carbon Additives	Current Collector	Areal Sulfur Loading (mg cm ⁻²)	Coin Cell Performance		Ref.
					Initial Capacity (mAh g ⁻¹)	Cycling Performance (mAh g ⁻¹)	
PVA-X	Sulfur/Carbon	~	Al foil	0.5	~	~	[34]
PVA	Sulfur/Carbon (super P)	~	Carbon paper	2.0/3.5/8.5/10.5	811 (at 0.2 C/10.5 mg cm ⁻²)	379 (at 0.2 C after 200 cycles) (10.5 mg cm ⁻²)	[35]
LiPAA-PVA	Sulfur/Carbon	Carbon black	Al foil	1.2	758.4 (at 0.25 C) (4.0 mg cm ⁻²)	646.9 (after 100 cycles) (4.0 mg cm ⁻²)	[36]

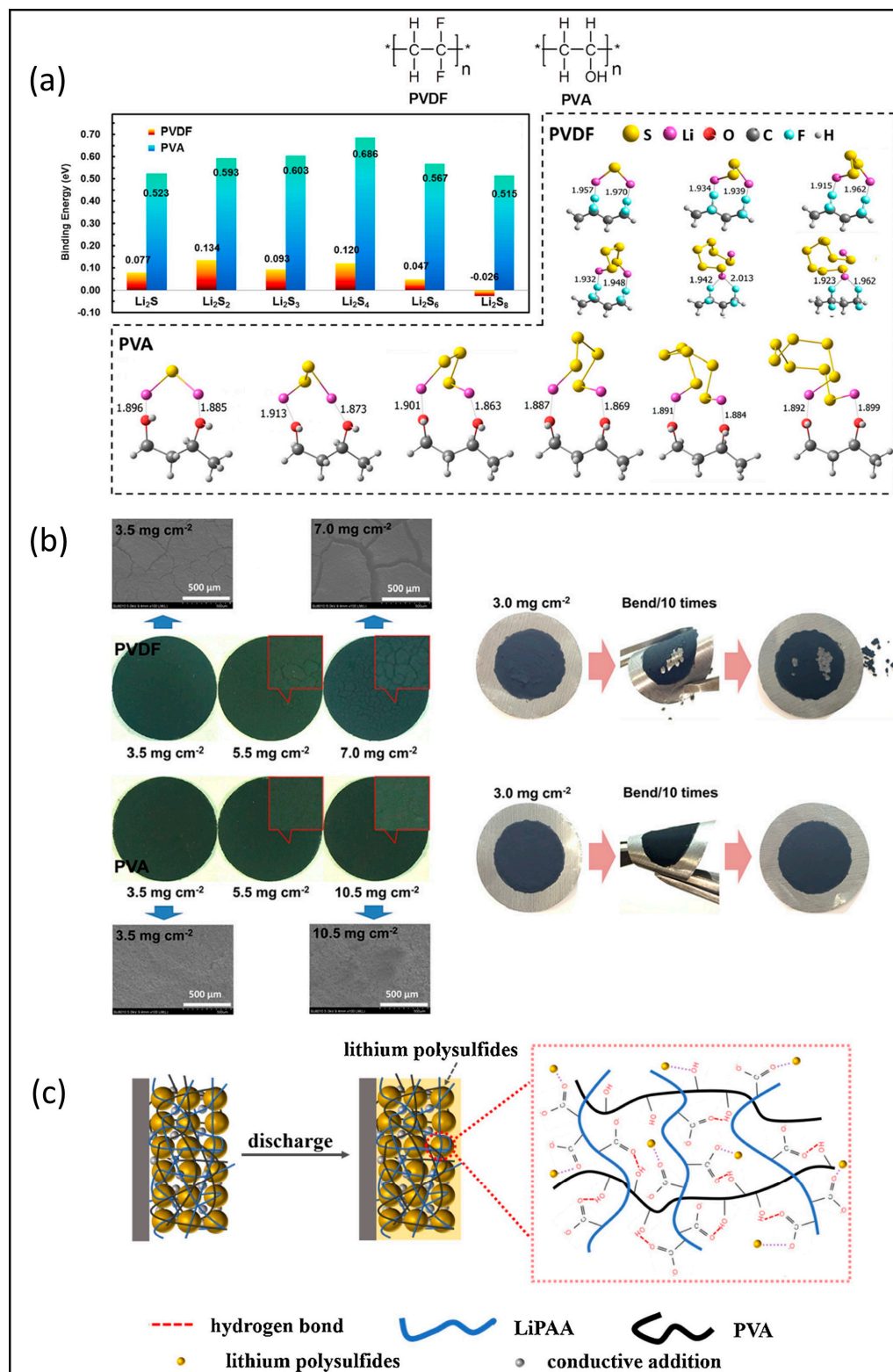


Figure 2. (a) Results from DFT calculations of PVDF and PVA with various lithium polysulfides; (b) optical microscopy, SEM images, and photographs of electrodes bound with PVA and PVDF. Reproduced with permission [35] Copyright 2020, American Chemical Society; (c) schematic representations of cathode configurations with LiPAA-PVA binder during electrochemical process. Reproduced with permission [36] Copyright 2020, Elsevier B.V.

2.3. Polyacrylic Acid (PAA) Binders

Polyacrylic acid dissolved in water at a neutral pH is an anionic polymer and is a well-known aqueous binder that was first used in sulfur cathode design in 2012 [37]. It provides a good cohesion between the active mass and conductive additives as well as adhesion between cathode materials and current collector. However, the swelling nature of PAA in molecular organic solvents, like the widely used battery solvent dimethoxyethane (DME), acts to weaken the adhesion strength between the cathode material and the current collector, which can lead to rapid capacity fading [37–39]. Subsequently, much effort has been devoted to solving the swelling problem without compromising the binders' performance. Pan et al. [38] fabricated a composite binder by combining poly(3,4-ethylenedioxythiophene)-poly(styrenesulfonate) (PEDOT:PSS) with PAA. The large amount of electrolyte absorbed by the PAA binder was confirmed, which indicated that the PAA binder was unsuitable in a sulfur cathode fabrication. But the PAA + PEDOT:PSS composite binder exhibited a moderate solvent uptake. The electrolyte swelling ability was easily controlled by adjusting the mass ratio between PAA and PEDOT:PSS. Also, the addition of PEDOT:PSS could provide enhanced electronic conductivity and polysulfide affinity. Polyacrylamide (PAM) was also blended with the PAA binder to mitigate swelling properties as well as to enhance the trapping of polysulfides through the amine group in PAM [40]. Fu's group included soy protein (SP) in the PAA binder system, fabricating a cross-linked SP-PAA network binder through the formation of hydrogen bonds [39]. The SP component exhibited strong polysulfide binding effects due to its abundant amine and carboxyl groups combined with good ion conductivity. A SP-PAA sulfur cathode with a sulfur loading of 5.6 mg cm^{-2} retained a specific capacity of 725 mAh g^{-1} after 100 cycles. Figure 3 shows other crosslinking network binders using PAA as the backbone, which have also been considered, including (a) PEI-PAA [41], hydroxypropyl polyrotaxane (HPRN+)-PAA [42], (b) xanthan gum/sodium polyacrylate/ Zn^{2+} [43], (c) ethanolamine-PAA [44], and (d) pectin (PEC)-PAA [45]. This cross-linking design improved the structural mechanical stability in sulfur cathodes, especially in thick coatings. As in the previous binder composites, the adsorption ability for polysulfides was enhanced by introducing various linking materials. Cathodes with a 5 mg cm^{-2} sulfur loading fabricated with an ethanolamine/PAA binder delivered a 679.0 mAh g^{-1} specific capacity at 0.2 C after 100 cycles [44]. Additionally, PAA showed the most promising performance in cells assembled with ionic liquid-containing electrolytes; their tested binders included PVDF, CMC:SBR, PAA, and LiPAA [46]. Kim's group [47] chose to use PAA with their sulfurized carbonized polyacrylonitrile cathode material. The cell with a 3.0 mg cm^{-2} sulfur loading exhibited a high initial capacity of 1500 mAh g^{-1} and a stable cycling performance of 98.5% capacity retention at 0.5 C after 100 cycles; however, this loading is lower than others reported here. Table 3 summarizes the composition and cycling performance of cathodes fabricated using a PAA binder.

Table 3. PAA binder in Li-S cathodes.

Binder	Cathode	Carbon Additives	Current Collector	Areal Sulfur Loading (mg cm^{-2})	Coin Cell Performance		Ref.
					Initial Capacity (mAh g^{-1})	Cycling Performance (mAh g^{-1})	
PAA	Sulfur	Super P	Al foil	1.5	758 (at 335 mA g^{-1})	325 (at 335 mA g^{-1} after 50 cycles)	[37]
PEDOT:PSS + PAA	Sulfur/Carbon (KB)	Acetylene black	Al foil	0.8	1121 (at 0.5 C)	833 (at 0.5 C after 80 cycles)	[38]
PAA	Sulfurized carbonized polyacrylonitrile (S-CPAN)	Super P	Carbon-coated Al foil	3	1530 (at 0.5 C)	1507 (at 0.5 C after 100 cycles)	[47]
SP-PAA	Sulfur	Carbon black	Carbon-coated Al foil	2.8/5.6/9.4	826 (at 0.3 A g^{-1}) (5.6 mg cm^{-2})	725 (at 0.3 A g^{-1} after 100 cycles)	[39]

Table 3. Cont.

Binder	Cathode	Carbon Additives	Current Collector	Areal Sulfur Loading (mg cm ⁻²)	Coin Cell Performance		Ref.
					Initial Capacity (mAh g ⁻¹)	Cycling Performance (mAh g ⁻¹)	
PAA-HPRN+	Sulfur/Super P	Acetylene black	Al foil	0.7/2.78/4.07	~	880.9 (at 0.2 C after 50 cycles) (4.07 mg cm ⁻²)	[42]
PAM-PAA	Sulfur/Carbon	Carbon black	Al foil	1.5–2	1008.1 (at 0.2 C)	600 (at 0.2 C after 200 cycles)	[40]
PAA-PEI	Sulfur/Carbon (KB)		Ni foam	5.5	1448 (at 0.1 C) (5.5 mg cm ⁻²)	841.7 (at 0.1 C after 100 cycles) (5.5 mg cm ⁻²)	[41]
NaPAA-XG/Zn	Sulfur/CNT	Super P	Carbon paper	1.2–1.5	~	770 (at 1 C after 300 cycles)	[43]
D-PAA/C-EA	Sulfur/Carbon (KB)	Acetylene black	Al foil/Carbon paper	1/3/5	~	679 (at 0.2 C after 100 cycles) (5 mg cm ⁻²)	[44]
PAA/PEC	Sulfur/PPy	Carbon black	Al foil	1.7/4.3	~	616 (at 0.2 C after 100 cycles) (4.3 mg cm ⁻²)	[45]

2.4. Polyethylene Oxide (PEO) Binders

Cheon's group first examined the structure and performance of sulfur cathode composed of sulfur, carbon, and a polyethylene oxide binder in 2002. As it exhibited a low capacity and poor cycling stability in a Li-S coin cell configuration [48], further efforts were subsequently devoted to fabricating PEO-mixed binders. For example, PEO and PVP mixed binders were used in both a Li₂S [49] and a sulfur cathode [50]. The addition of PVP in the PEO binder facilitates the coating of the aqueous slurry and improves the capacity stability due to the amine groups present in the PVP binder component. Matthew's group also examined similar binder systems with a polyether component [50], as shown in Figure 4a. The cathodes with ~2 mg cm⁻² sulfur loading preserved the electrochemical performance with ~900 mAh g⁻¹ under 0.1 C. However, there are some drawbacks for this mixed-binder system due to the fact that PEO and PVP show only limited miscibility. When it occurs, phase separation leads to performance degradation and/or inefficient material utilization. In addition, the viscosity of the cathode slurry is increased when using porous C/S composites [51]. To overcome this issue, Yu-Chuan Chien et al. synthesized a series of poly (ethylene glycol-block-2-ethyl-2-oxazoline) binders with various block lengths, which contained both the polyether functionality of PEO and the amide functionality of PVP [51]. Cathodes composed of this co-polymer binder only exhibited electrochemical performance comparable to a PEO + PVP mixture. Yu's group fabricated a 3D crosslinked tannic acid (TA)-PEO complex as the binder in Li-S cathodes, and the polymer structure is shown in Figure 4b [52]. At a sulfur loading of 5.0 mg cm⁻², the cell delivers a capacity retention of 74.5% over 150 cycles. By inducing branched PEI and citric acid (CA) into the PEO + PVP system, a cross-linked PEI-PVP-CA-PEO network was developed by Do et al. [53], with the structure shown in Figure 4c. They obtained an integrated cathode coating with a high sulfur loading of 10 mg cm⁻²; however, they only reported the performance for a 6 mg cm⁻² sulfur loading, for which they achieved a stable capacity around 400 mAh g⁻¹ for 200 cycles at 1 C. Wang's group [54] built a conductive network composed of a phosphorylated soy protein isolate (P-SPI), PEO, and phytic acid (PA) with PEDOT:PSS, where the binder formation diagram is shown in Figure 4d. Using this binder, the cathode with a sulfur loading similar to the composite of Do et al. (6.1 mg cm⁻²) delivered a capacity of 800 mAh g⁻¹ after 50 cycles, albeit at lower cycling rate of 0.1 C. The coin cell performances of the mentioned cathodes are summarized in Table 4.

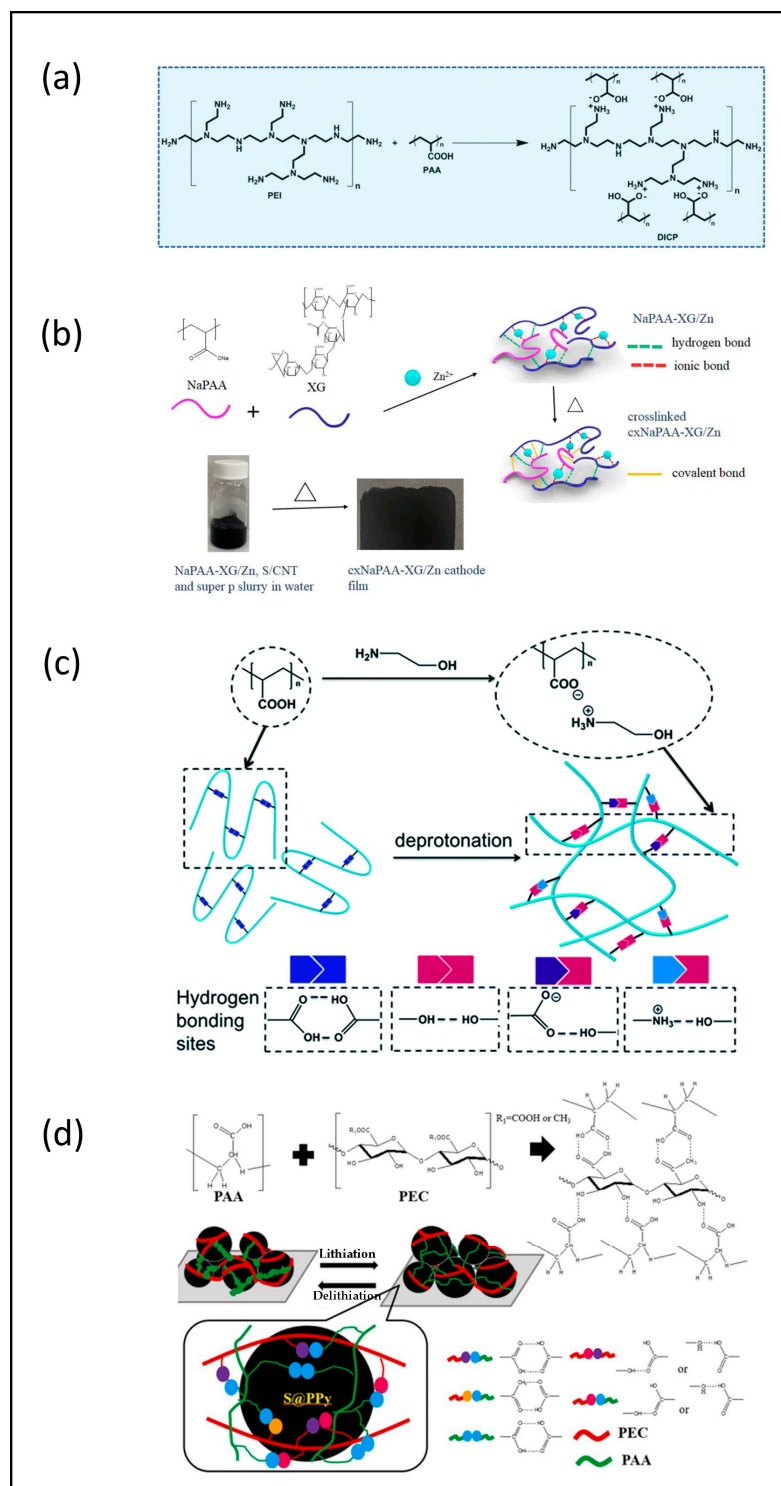


Figure 3. (a) Synthesis scheme of DICP through carboxy-amino ionic interaction between PAA and PEI. Reproduced with permission [41] Copyright 2020, WILEY-VCH; (b) reaction of NaPAA, XG, and Zn^{2+} to form triple cross-linked $cxNaPAA-XG/xZn$ binders and the digital images of the homogeneous dispersion of NaPAA-XG/Zn, S/CNT, and Super P slurry in water and the $cxNaPAA-XG$ cathode film. Reproduced with permission [43] Copyright 2021, American Chemical Society; (c) schematic illustration of the deprotonation process, reproduced with permission [44], Copyright 2021, The Royal Society of Chemistry; (d) H bond interactions to form PAA/PEC_(x) binders, which contain varieties of H bond interactions among cathode components to provide mechanical strength and interfacial adhesion of the cathode during lithiation/de-lithiation cycles. Reproduced with permission [45] Copyright 2022, Elsevier Ltd.

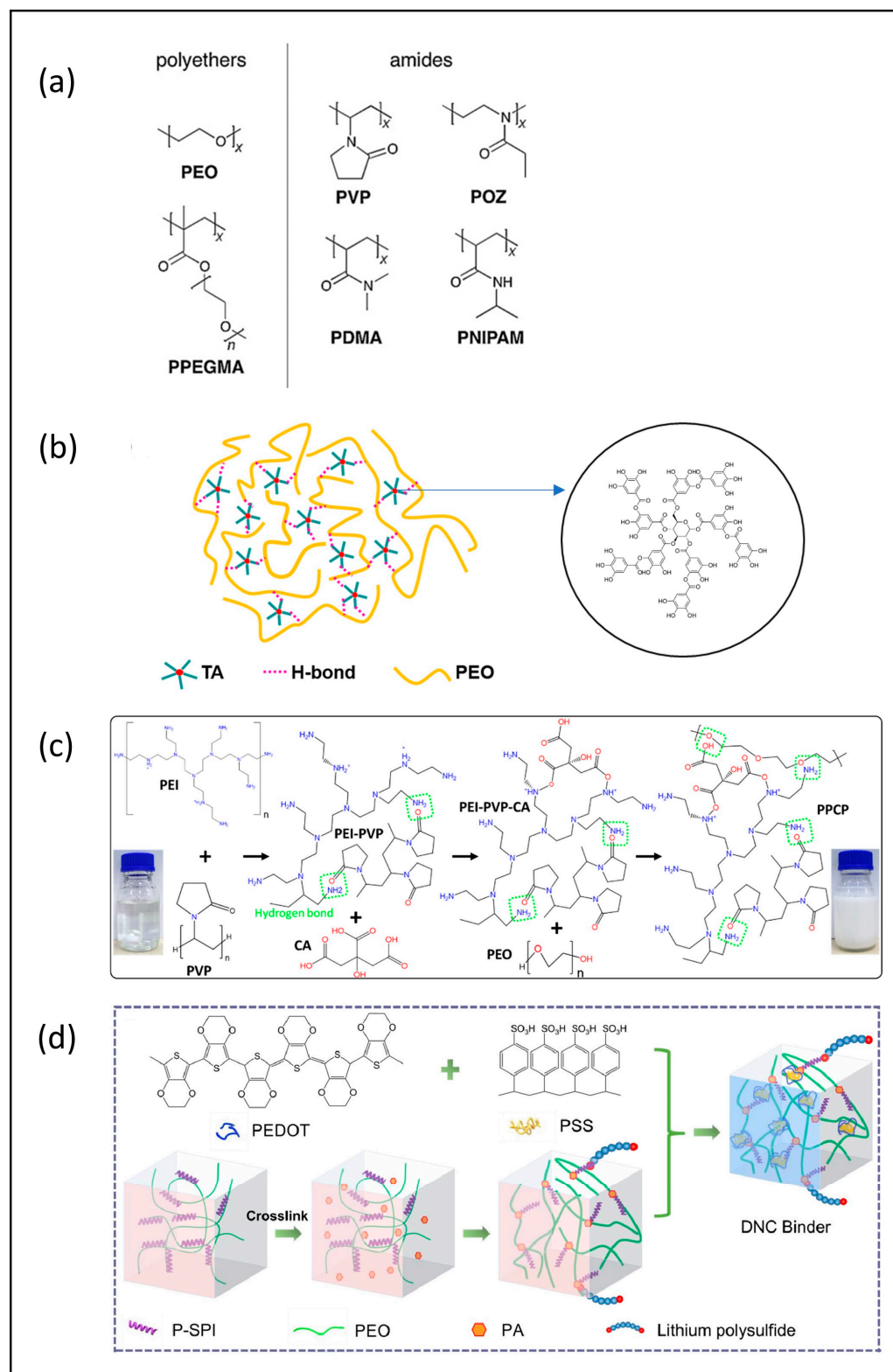


Figure 4. (a) Structures of the candidate binders investigated. Reproduced with permission [50], Copyright 2017, Wiley-VCH; (b) chemical structures of TA, PEO, and TA/PEO. Reproduced with permission [52], Copyright 2018, Elsevier B.V.; (c) material design and structure of the multifunctional PPCP binder. Reproduced with permission [53], Copyright 2022, American Chemical Society; (d) schematic diagram of the formation of DNC binder. Reproduced with permission [54], Copyright 2021, Elsevier Ltd.

Table 4. PEO binder in Li-S cathodes.

Binder	Cathode	Carbon Additives	Current Collector	Areal Sulfur Loading (mg cm ⁻²)	Coin Cell Performance		Ref.
					Initial Capacity (mAh g ⁻¹)	Cycling Performance (mAh g ⁻¹)	
PEO	Sulfur	Super P	Al foil	1.5	~	~	[48]
PEO + PVP	Li2S/KB	Acetylene black	Al foil	1.5	~	460 (at 0.1 C after 50 cycles)	[49]
PEO + PVP	Sulfur/KB	VGCF/Super C65	Graphite-coated Al foil	1.9–2.2	~	900 (at 0.1 C after 50 cycles) (1.2 mg cm ⁻²)	[50]
PEO-TA	Sulfur/Carbon (Super P)	~	Ni foam	2.0/3.0/4.0/5.0	1051.5 (at 0.2 C)	~400 (at 0.2 C after 150 cycles) (5 mg cm ⁻²)	[52]
poly (ethylene glycol-block-2-ethyl-2-oxazoline)	Sulfur/KB	VGCF/Super C65	Carbon-coated Al foil	2.01–2.44	1250 (at 0.04 C)	950 (at 0.04 C after 75 cycles) (~2 mg cm ⁻²)	[51]
PEDOT:PSS/P-SP/PEO/PA	Sulfur/Carbon (3D carbon)	Super P	Carbon-coated Al foil	1.2/1.7/3.6/4.5/6.1	969.1 (at 1 C) (1.2 mg cm ⁻²)	664.0 (at 1 C after 500 cycles)	[54]
PEI-PVP-PEO	Sulfur/MWCNT	Carbon black/carbon fiber	Al foil	2.5–10	981.6 (at 0.5 C) (2.5 mg cm ⁻²)	598 (at 0.5 C) after 200 cycles	[53]

2.5. Polyethylene Imine (PEI) Binders

Polyethylene imine is a polymer with repeating units composed of the amine group and two carbon aliphatic $-\text{CH}_2\text{CH}_2-$ spacers. It has been widely used as a cationic dispersant to stabilize aqueous suspensions and additives to promote the adhesion of paints, inks, and pigments to different surfaces. Linear polar PEI was applied to develop high-performance sulfur cathodes as a functional binder by Zhang's group [55] and Liao's group [56]. Both confirmed the enhanced binding strength of PEI relative to PVDF and the strong electrostatic interaction between amino groups and lithium polysulfide intermediates, as shown in Figure 5a, and enhanced electrochemical performance compared with a similar sulfur cathode using PVDF binder, as shown in Figure 5b. It is worth noting that different sulfur host materials are used for PVDF and PEI-based electrodes. Zhang's group obtained a thick cathode with 8.6 mg cm⁻² sulfur loading and achieved a 744.2 mAh g⁻¹ capacity after 50 cycles at 0.05 C [55]. While the cathode of Liao's group with a sulfur loading of 6.5 mg cm⁻² delivered 509 mAh g⁻¹, it is important to note that this performance was achieved at a 10-times-higher rate of 0.5 C and after 170 cycles. The modification of PEI was also considered in the binder design for sulfur cathodes, for example, gelatine-PEI composite [57], CH₃I-PEI [58], and cross-linked PVP-PEI [59], but there was no obvious performance improvement in thick cathodes with these modified PEI binders. Table 5 includes the detailed performance of cathodes using PEI binders.

Table 5. PEI binder in Li-S cathodes.

Binder	Cathode	Carbon Additives	Current Collector	Areal Sulfur Loading (mg cm ⁻²)	Coin Cell Performance		Ref.
					Initial Capacity (mAh g ⁻¹)	Cycling Performance (mAh g ⁻¹)	
PEI	Sulfur	Super C45/graphene	Al foil	8.6	1126.4 (at 0.05 C) (8.6 mg cm ⁻²)	744.2 (at 0.05 C after 50 cycles)	[55]
Gelatin-PEI	Sulfur	Acetylene black	Al foil	1.07–3.2	969.4 (at 0.2 C) (2.14 mg cm ⁻²)	845.7 (at 0.2 C after 50 cycles)	[57]
PEI	Sulfur/Super P	Super P	Carbon paper	2.4/3.5/5.5/6.5	1089 (at 0.5 C) (3.5 mg cm ⁻²)	554 (at 0.5 C after 300 cycles) 509 (at 0.5 C after 170 cycles) (6.5 mg cm ⁻²)	[56]

Table 5. Cont.

Binder	Cathode	Carbon Additives	Current Collector	Areal Sulfur Loading (mg cm^{-2})	Coin Cell Performance		Ref.
					Initial Capacity (mAh g^{-1})	Cycling Performance (mAh g^{-1})	
PEI cationic polymer (CH_3I)	Sulfur	Super C45/graphene	Al foil	6.5	~	~670 (at 0.05 C after 70 cycles)	[58]
PVP-PEI	Sulfur/Carbon	Carbon black	Al foil/carbon paper	1.5–3.32	1481 (at 0.5 C) (2 mg cm^{-2})	880.1 (at 0.5 C after 150 cycles)	[59]

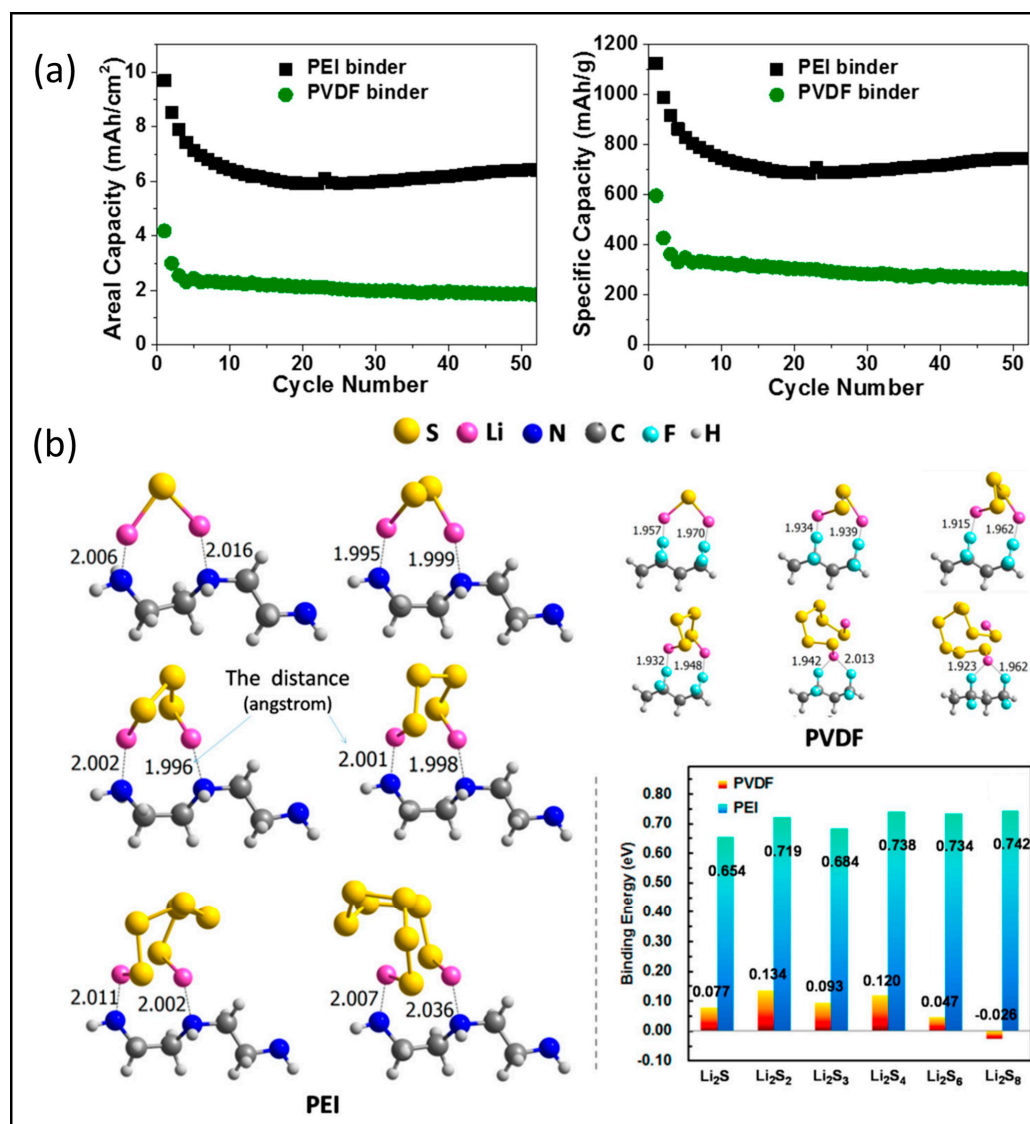


Figure 5. (a) Cycling behavior of PEI- and PVDF-based sulfur cathodes at a current density of 0.05 C. Reproduced with permission [55], Copyright 2017, Elsevier Ltd.; (b) DFT calculation results of PEI in contact with various polysulfides. Reproduced with permission [56], Copyright 2018, American Chemical Society.

2.6. Other Functional Aqueous Binders

In addition to the most common aqueous binders listed above, several other functional binders have been studied by some researchers, and a summary of their performance is presented in this section. Zhang's group designed a 3D network binder by combining two biopolymers of guar and xanthan gums using the intermolecular binding effect between

the functional groups in both polymers [60]. Based on the conclusion the authors drew from their FTIR spectroscopic investigation of the mixture of Gum arabic and polysulfides, the large amount of oxygen-containing functional groups in both polymers can effectively bind with polysulfides, and the robust network can provide a strong support to the active materials. They achieved a sulfur loading of 19.8 mg cm^{-2} and an areal capacity of 26.4 mAh cm^{-2} , but effective cycling only survived 5 cycles with this extremely high sulfur loading. For a cathode with a lower sulfur loading (11.9 mg cm^{-2}), they obtained a stable capacity of 800 mAh g^{-1} for 50 cycles at 1.6 mA cm^{-2} . Jie et al. exploited the advantage of the crosslinking effect of sodium alginate (SA) and Cu^{2+} ions to prepare a SA-Cu binder [61]. They proposed that both the oxygen-containing functional groups of SA and Cu^{2+} could interact with the polysulfide anions, which may suppress the shuttle effect. The binding energy of nine different functional groups with Li_2S_6 is shown in Figure 6a. Additionally, they proposed that this network hinders large volume changes during the charge–discharge process. Using this binder, a cathode with a sulfur loading of 8.05 mg cm^{-2} was obtained and delivered a capacity of 892 mAh g^{-1} at 1.0 mA cm^{-2} but only for 30 cycles. Liu et al. synthesized a double-chain polymer network (DCP) binder by polymerizing 4,4'-biphenyl disulfonic acid connecting a pyrrole monomer onto a viscous CMC matrix, as in Figure 6b [62]. The capacity of the cathode with a 9.8 mg cm^{-2} sulfur loading using this binder was below 600 mAh g^{-1} at 0.5 mA cm^{-2} after 50 cycles. Jin et al. synthesized a bioinspired water-based 3D network binder (DSM) through a one-step free radical solution polymerization of N-(3,4-dihydroxyphenethyl) acrylamide (DAA), 2-methacryloyloxy ethyl dimethyl-3-sulfopropyl ammonium hydroxide (SBMA), and poly (ethylene glycol) methyl ether methacrylate (PEGMA) [63]. They suggested that the negatively charged sulfonate coordination sites could induce fast lithium-ion diffusion in the cathode. A cathode with a sulfur loading of 9.7 mg cm^{-2} retained a capacity of 721 mAh g^{-1} during 70 cycles, and a cathode with the highest sulfur loading of 12 mg cm^{-2} could be cycled for 30 cycles under 0.5 C. Chu et al. reported a binder comprising chitosan grafted with a catechol moiety for sulfur cathodes [64]. The cathode had a 600 mAh g^{-1} capacity with a 4.3 mg cm^{-2} sulfur loading, but when the loading increased to 12.2 mg cm^{-2} , the capacity dropped below 100 mAh g^{-1} as shown in Figure 6c. Rashid et al. coated a uniform nano super-adhesion polydopamine (PD) on the graphene sulfur (G-S) surface and then used a cross-linked polyacrylamide (c-PAM) binder. The synthesis process is shown in Figure 6d, which could provide affinity with the PD coating, thus tightly integrating sulfur with the binder network and greatly boosting the overall mechanical strength/conductivity of the electrode [65]. This G-S@PD-cPAM cathode with a sulfur loading of 9.1 mg cm^{-2} maintained a capacity of 396 mAh g^{-1} after 50 cycles at 0.2 C. Table 6 summarizes the details and performance of these cathodes with various functional aqueous binders.

Table 6. Other functional aqueous binders of highly loaded sulfur cathodes.

Binder	Cathode	Carbon Additives	Current Collector	Areal Sulfur Loading (mg cm^{-2})	Coin Cell Performance		Ref.
					Initial Capacity (mAh g^{-1})	Cycling Performance (mAh g^{-1})	
N-GG-XG binder (guar gum (GG) and xanthan gum (XG))	Sulfur/Carbon (super P)	Ni foam	6.5/11.9/19.8	1200	724 (at 0.5 C after 150 cycles) (0.78 mg cm^{-2})	733 (at 1.6 mA cm^{-2} after 60 cycles) (11.9 mg cm^{-2})	[60]
SA-Cu	Sulfur/Carbon (super P)	Carbon cloth	0.75/4.1/8.05	1200	758 (at 1 C after 250 cycles) (0.75 mg cm^{-2})	598 (at 0.15 C after 60 cycles) (4.1 mg cm^{-2})	[61]
DCP (4,4'-biphenyldisulfonic acid (BSA) connected pyrrole monomer)	Sulfur/Carbon (CNT)	Ni foam	2.5/5.2/6.8/9.8	1326.9	649.2 (at 1.5 C after 400 cycles) (1.2 mg cm^{-2})	600 (at 0.5 mA cm^{-2} after 50 cycles) (9.8 mg cm^{-2})	[62]

Table 6. Cont.

Binder	Cathode	Carbon Additives	Current Collector	Areal Sulfur Loading (mg cm ⁻²)	Coin Cell Performance		Ref.
					Initial Capacity (mAh g ⁻¹)	Cycling Performance (mAh g ⁻¹)	
P(DAA-r-SBMA-r-PEGMA) (DSM)	Sulfur/Carbon (super P)	Ni foam	3.7/6.6/9.7/12.0	1077	674.2 (at 1 C after 350 cycles)	742.3 (at 0.81 mA cm ⁻² after 70 cycles) (9.8 mg cm ⁻²)	[63]
CN (chitosan substituted with nitrocatechol)	Sulfur	Ni foam/Al foil	2.0/3.7/4.3/11.3/12.2	902.2	~	700 (at 0.2 C after 100 cycles) (4.3 mg cm ⁻²)	[64]
PD-c-PAM (polydopamine cross-linked polyacrylamide)	Graphene/Sulfur	Al foil	2.2/4.5/7.0/8.2/9.1	1145	495 (at 4 C after 800 cycles) (2.0 mg cm ⁻²)	480 (at 1 C after 300 cycles) (5.6 mg cm ⁻²)	[65]

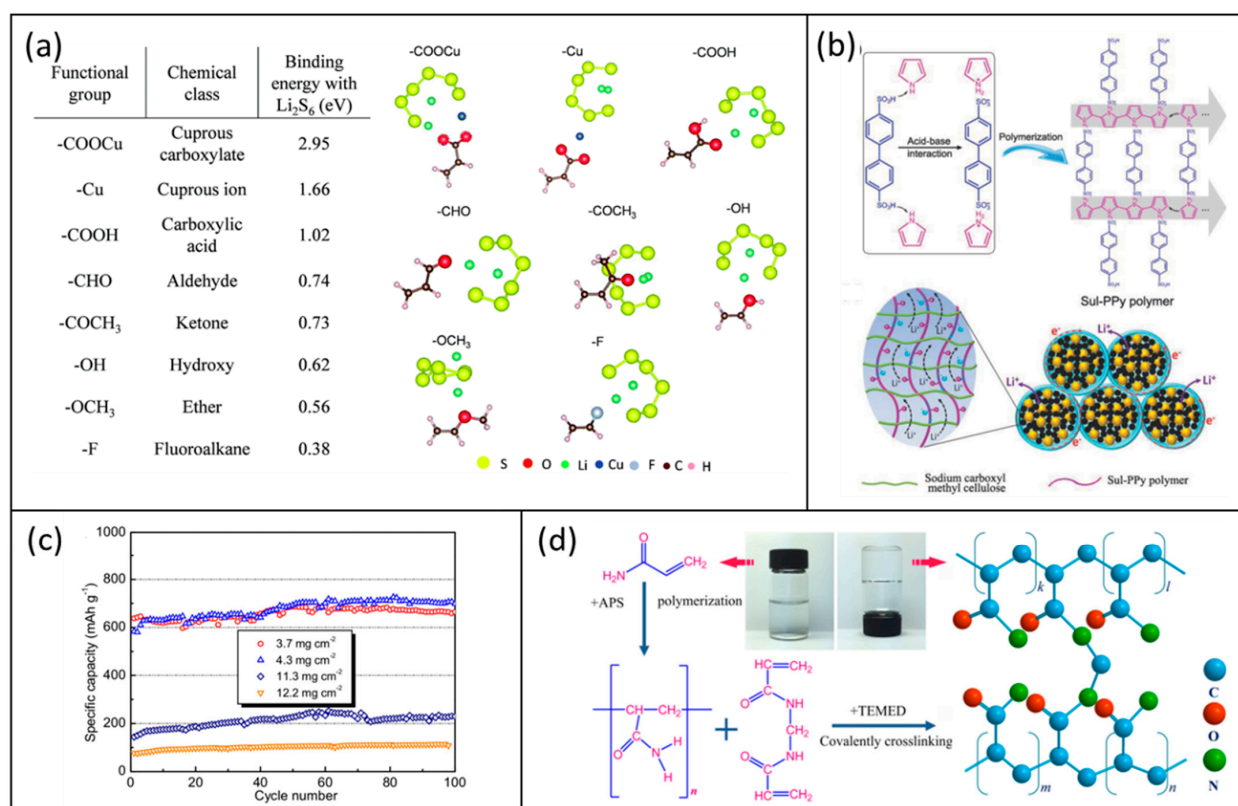
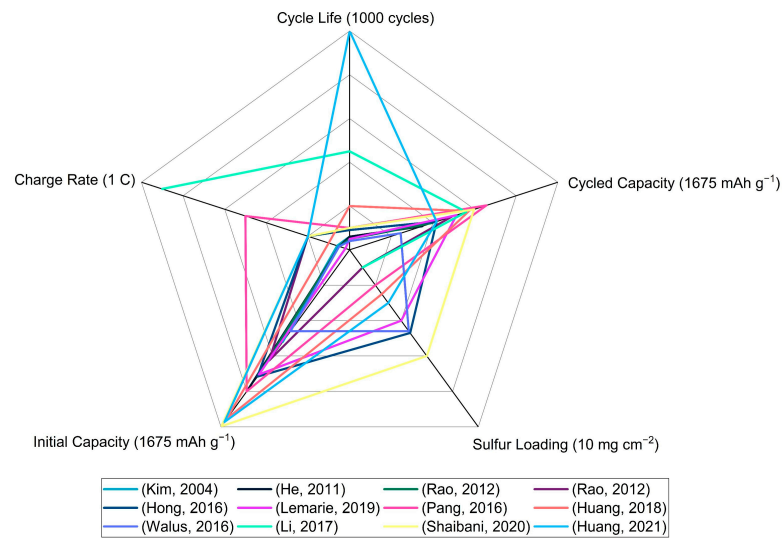


Figure 6. (a) Binding energies of Li_2S_6 with various functional groups. Reproduced with permission [61], Copyright 2018, The Royal Society of Chemistry; (b) chemical oxidative polymerization of 4,4-biphenyldisulfonic acid connected pyrrole, producing crystalline Sul-PPy polymers. Reproduced with permission [62], Copyright 2018, WILEY-VCH; (c) cycling performances of the cathodes with different sulfur loadings at 0.2. Reproduced with permission [64], Copyright 2019, Elsevier B.V.; (d) schematic illustration showing the synthetic process of the high-strength cross-linked c-PAM hydrogel binder. Reproduced with permission [65], Copyright 2020, Elsevier B.V.

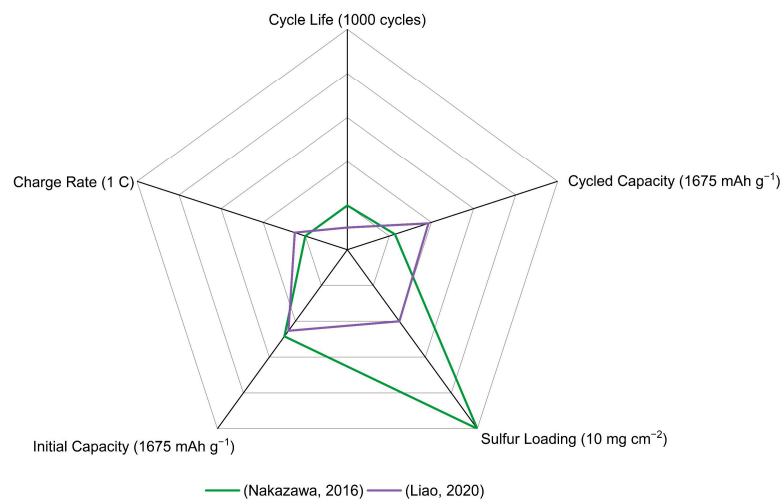
3. Conclusions

In this review, there is a systematic summary of the status of five commercially available aqueous-based binders that are used in Li-S batteries, namely, CMC, PVA, PAA, PEO, and PEI, as well as details of some other synthesized functional binders. The key parameters of electrode performance, cycle life, charge rate, cycled capacity, initial capacity, and sulfur loading are compared so as to provide an evaluation of binder performance. A graphical summary is presented in Figure 7.

(a) CMC



(b) PVA



(c) PAA

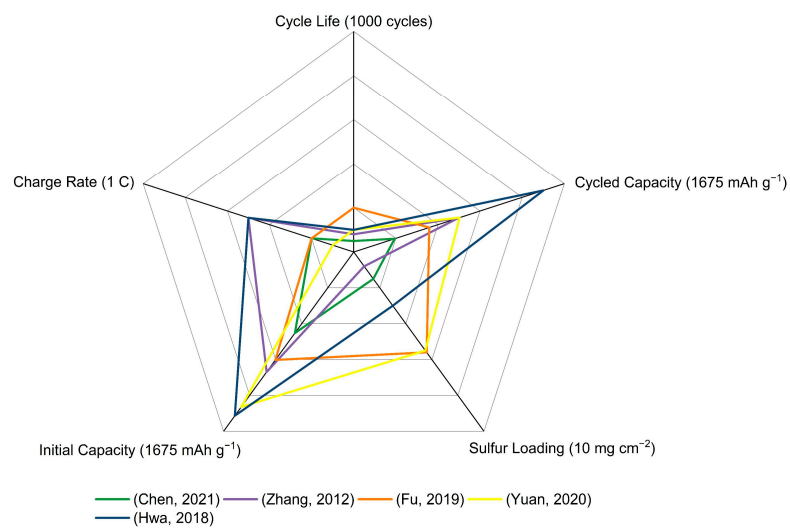
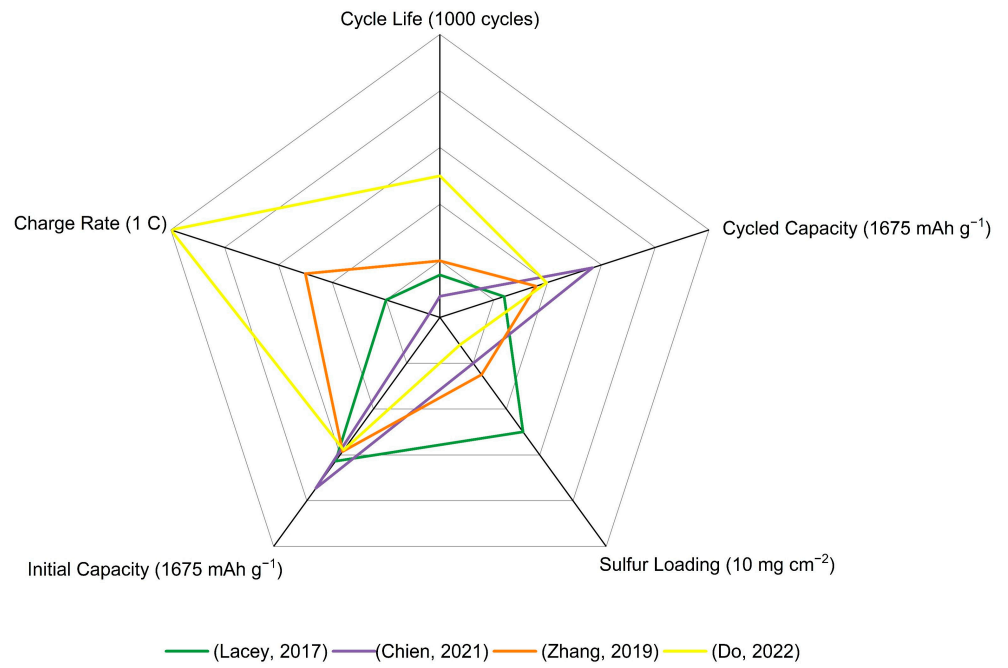


Figure 7. Cont.

(d) PEO



(e) PEI

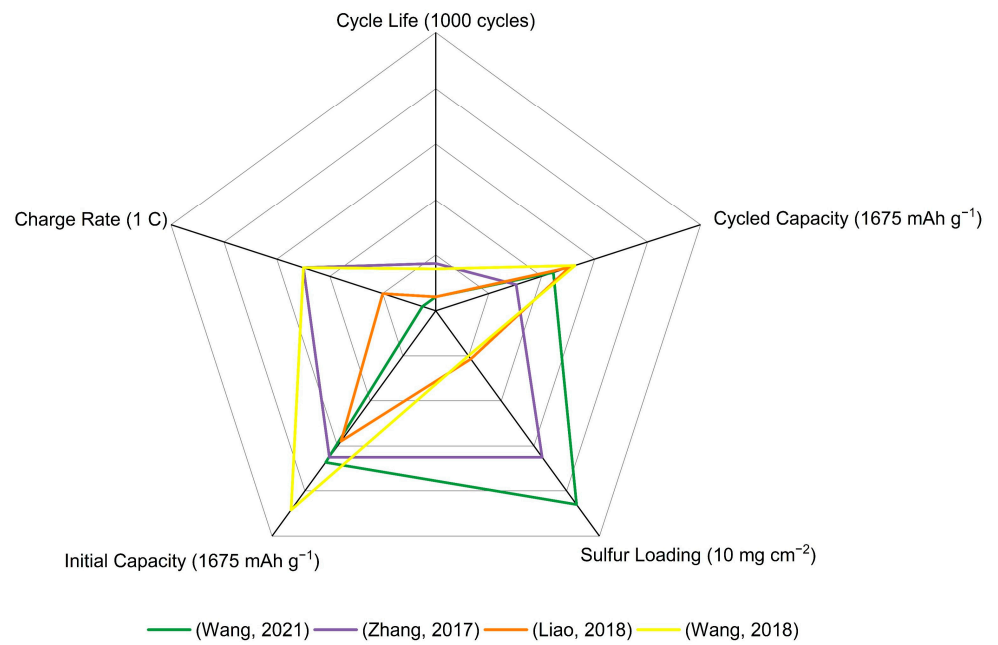
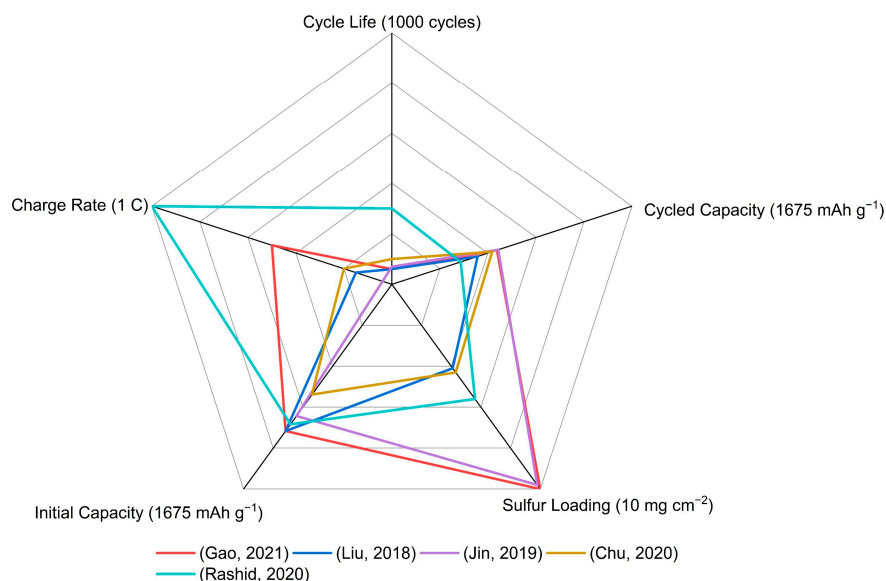


Figure 7. Cont.

(f) Other functional aqueous binders



(g) Performance comparison of representative binders

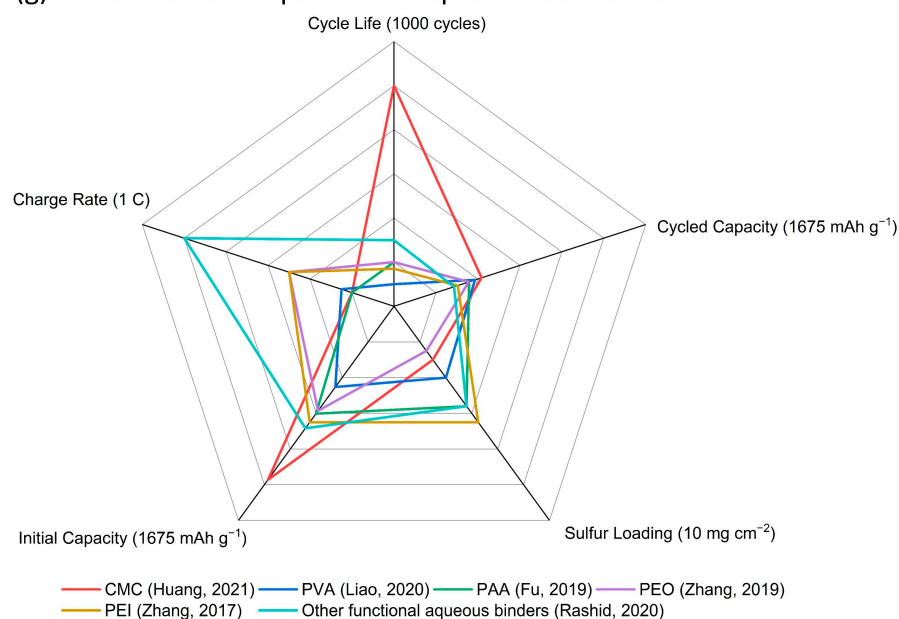


Figure 7. Radar graphs of (a) CMC (Kim, 2004) [20], (He, 2011) [21], (Rao, 2012) [22], (Rao, 2012) [23], (Hong, 2016) [24], (Lemarie, 2019) [26], (Pang, 2016) [27], (Huang, 2018) [28], (Walus, 2016) [29], (Li, 2017) [30], (Shaibani, 2020) [31], (Huang, 2021) [32], (b) PVA (Nakazawa, 2016) [34], (Liao, 2020) [35], (c) PAA (Chen, 2021) [36], (Zhang, 2012) [37], (Fu, 2019) [39], (Yuan, 2020) [40], (Hwa, 2018) [46], (d) PEO (Lacry, 2017) [50], (Chien, 2021) [51], (Zhang, 2019) [52], (Do, 2022) [53], (e) PEI (Wang, 2021) [54], (Zhang, 2017) [55], (Liao, 2018) [56], (Wang, 2018) [58], (f) other functional aqueous binders (Gao, 2021) [59], (Liu, 2018) [61], (Jin, 2019) [63], (Chu, 2020) [64], (Rashid, 2020) [65], and (g) performance comparison of representative binders in the above aqueous binder system with sulfur loading above 5 mg cm^{-2} (Huang, 2021) [32], (Liao, 2020) [35], (Fu, 2019) [39], (Zhang, 2019) [52], (Zhang, 2017) [55], (Rashid, 2020) [65].

It is hard to compare the electrochemical performance objectively due to the various conditions such as the electrode materials, cell assembly design, and test conditions. However, this large survey of data does allow for the key features of these binders to be assessed and then linked to recommendations for use. CMC serving as a binder itself, along with SBR, and cross-linked by CA, has been extensively explored in sulfur cathodes, and improvements in cathode capacity and cycling stability compared with similar cathodes using a PVDF binder have been confirmed by several research groups. The use of CMC + SBR and cross-linked CMC–CA have allowed for sulfur cathodes with the highest loadings to be fabricated. PVA has been explored with a view to the enhancement of polysulfide retention in the cathode structure through its hydroxy-group functionality. Although the PVA binders have proven to provide enough binding energy in thick cathodes, there is no obvious improvement in electrochemical performance. Sulfur cathodes with PAA binders suffer from swelling problems in the common ether-based electrolyte solvents. A large amount of work has been undertaken to add other components, including PEDOT:PSS and PAM in PAA, or to fabricate cross-linking systems, such as SP–PAA, PEI–PAA, HPRN⁺–PAA, ethanolamine–PAA, and PEC–PAA, to adjust the swelling level and build highly loaded cathodes. Based on the results, the swelling ability was controlled, and the high sulfur loading (maximum 9.4 mg cm^{−2}) was achieved. However, no clear improvement in electrochemical performance was found. A range of PEO-containing formulations has been trialed as binders: from simple PEO + PVP mixtures to polyether component and amide-containing component binder systems, poly (ethylene glycol-block-2-ethyl-2-oxazoline) with both the polyether functionality of PEO and the amide functionality of PVP, and then to more complex cross-linked TA–PEO, PEI–PVP–CA–PEO, and PEDOT:PSS/P-SP/PEO/PA combinations. However, none of these led to any significant electrochemical enhancements in highly loaded sulfur cathodes. PEI with amino groups and a strong electrostatic interaction with lithium polysulfide intermediates were used in some thick sulfur cathodes exhibiting similar performance with other binders such as PAA and PEO. In addition, some other synthesized aqueous-based polymer binders used in Li-S batteries are also included in this review. The main improvements for these functional binders can be summarized as follows: (i) polar groups for good binding strength; (ii) cross-linked networks for stable mechanical structure; (iii) functional groups for lithium polysulfides trapping; (iv) addition of conductive components for improved electron and ion conductivity. Different functional groups including –OH, –COOH, –SO₃H, and –SO₃Li have acted as the polysulfide-interacting sites in highly loaded sulfur cathodes, which has exhibited improved performance, but considering the complicated fabrication process for these binders, any practical application in Li-S batteries seems unlikely.

Based on the above summary and comparison of the aqueous binders, some commercial aqueous binders have shown promise for fabricating high-performance or high-sulfur-loading cathodes at a laboratory level in Li-S batteries. However, it is still very challenging to simultaneously achieve high capacity and long cycling stability for highly loaded sulfur cathodes using commercial water-based binders. While some functional water-based binders prepared in laboratories exhibit excellent performance with high sulfur loading, their complex and costly production processes highlight the need for further optimization in both manufacturing and cost-efficiency for industrial-scale applications. Moreover, the swelling nature for these binders (except PAA, as noted earlier) has not been fully studied or considered in most cathode designs. Based on these commercial products, the modification method for a highly loaded cathode is still unclear, and the mechanism should be further explored. Certainly, to maintain the integrity and active material utilization of thick cathodes is not only dependent on these binders but also other improvements for host materials, carbon additives, current collectors, electrolyte, and separators. Meanwhile, pouch cell performance with a highly loaded sulfur cathode should be further expanded in battery testing to evaluate the scalability (complexity, cost, and stable electrochemical cycling) of these reported sulfur cathodes. Such comprehensive

research efforts are essential for propelling the commercialization of Li-S battery technology and directing future research paths.

Author Contributions: Conceptualization, W.W.; paper collection, W.W.; analysis, W.W.; writing—original draft preparation, W.W.; writing—review and editing, M.B., A.F.H., and P.J.M.; supervision, M.B. and P.J.M. All authors have read and agreed to the published version of the manuscript.

Funding: This work was funded by CSIRO's Space Technology Future Science Platform.

Data Availability Statement: This paper contains no supporting data.

Acknowledgments: The authors acknowledge the support from staff members at CSIRO, Manufacturing, Materials Characterization and Modelling Program.

Conflicts of Interest: The authors declare no conflicts of interest.

References

1. Yin, Y.X.; Xin, S.; Guo, Y.G.; Wan, L.J. Lithium-sulfur batteries: Electrochemistry, materials, and prospects. *Angew Chem. Int. Ed. Engl.* **2013**, *52*, 13186–13200. [[CrossRef](#)]
2. Lu, Y.; Zhang, Q.; Chen, J. Recent progress on lithium-ion batteries with high electrochemical performance. *Sci. China Chem.* **2019**, *62*, 533–548. [[CrossRef](#)]
3. Fichtner, M. Recent research and progress in batteries for electric vehicles. *Batter. Supercaps.* **2021**, *5*, e202100224. [[CrossRef](#)]
4. Deng, J.; Bae, C.; Denlinger, A.; Miller, T. Electric vehicles batteries: Requirements and challenges. *Joule* **2020**, *4*, 511–515. [[CrossRef](#)]
5. Tian, Y.; Zeng, G.; Rutt, A.; Shi, T.; Kim, H.; Wang, J.; Koettgen, J.; Sun, Y.; Ouyang, B.; Chen, T.; et al. Promises and challenges of next-generation “beyond Li-ion” batteries for electric vehicles and grid decarbonization. *Chem. Rev.* **2021**, *121*, 1623–1669. [[CrossRef](#)] [[PubMed](#)]
6. Ye, Z.; Jiang, Y.; Li, L.; Wu, F.; Chen, R. Rational design of MOF-based materials for next-generation rechargeable batteries. *Nano-Micro Lett.* **2021**, *13*, 203. [[CrossRef](#)] [[PubMed](#)]
7. Cleaver, T.; Kovacic, P.; Marinescu, M.; Zhang, T.; Offer, G. Perspective—Commercializing lithium sulfur batteries: Are we doing the right research? *J. Electrochem. Soc.* **2017**, *165*, A6029–A6033. [[CrossRef](#)]
8. Hu, Y.; Chen, W.; Lei, T.; Jiao, Y.; Huang, J.; Hu, A.; Gong, C.; Yan, C.; Wang, X.; Xiong, J. Strategies toward high-loading lithium-sulfur battery. *Adv. Energy Mater.* **2020**, *10*, 2000082. [[CrossRef](#)]
9. Bhargava, A.; He, J.; Gupta, A.; Manthiram, A. Lithium-sulfur batteries: Attaining the critical metrics. *Joule* **2020**, *4*, 285–291. [[CrossRef](#)]
10. Zhang, G.; Zhang, Z.W.; Peng, H.J.; Huang, J.Q.; Zhang, Q. A toolbox for lithium-sulfur battery research: Methods and protocols. *Small Methods* **2017**, *1*, 1700134.
11. Rana, M.; Ahad, S.A.; Li, M.; Luo, B.; Wang, L.; Gentle, I.; Knibbe, R. Review on areal capacities and long-term cycling performances of lithium sulfur battery at high sulfur loading. *Energy Storage Mater.* **2019**, *18*, 289–310. [[CrossRef](#)]
12. Zhou, H.-J.; Song, C.-L.; Si, L.-P.; Hong, X.-J.; Cai, Y.-P. The development of catalyst materials for the advanced lithium-sulfur battery. *Catalysts* **2020**, *10*, 682. [[CrossRef](#)]
13. Zhao, H.; Deng, N.; Yan, J.; Kang, W.; Ju, J.; Ruan, Y.; Wang, X.; Zhuang, X.; Li, Q.; Cheng, B. A review on anode for lithium-sulfur batteries: Progress and prospects. *J. Chem. Eng.* **2018**, *347*, 343–365. [[CrossRef](#)]
14. Brückner, J.; Thieme, S.; Grossmann, H.T.; Dörfler, S.; Althues, H.; Kaskel, S. Lithium-sulfur batteries: Influence of c-rate, amount of electrolyte and sulfur loading on cycle performance. *J. Power Sources* **2014**, *268*, 82–87. [[CrossRef](#)]
15. Li, J.-T.; Wu, Z.-Y.; Lu, Y.-Q.; Zhou, Y.; Huang, Q.-S.; Huang, L.; Sun, S.-G. Water soluble binder, an electrochemical performance booster for electrode materials with high energy density. *Adv. Energy Mater.* **2017**, *7*, 1701185. [[CrossRef](#)]
16. Liao, J.; Wang, J.; Liu, Z.; Ye, Z. Polar benzimidazole-containing (sulfonated) poly(arylene ether ketone)s as bifunctional binders for lithium-sulfur battery cathodes with high sulfur loadings. *ACS Appl. Energy Mater.* **2019**, *2*, 6732–6740. [[CrossRef](#)]
17. Liu, J.; Zhang, Q.; Sun, Y.-K. Recent progress of advanced binders for Li-S batteries. *J. Power Sources* **2018**, *396*, 19–32. [[CrossRef](#)]
18. Bresser, D.; Buchholz, D.; Moretti, A.; Varzi, A.; Passerini, S. Alternative binders for sustainable electrochemical energy storage—the transition to aqueous electrode processing and bio-derived polymers. *Energy Environ. Sci.* **2018**, *11*, 3096–3127. [[CrossRef](#)]
19. Jin, B.; Li, Y.; Qian, J.; Zhan, X.; Zhang, Q. Environmentally friendly binders for lithium-sulfur batteries. *ChemElectroChem* **2020**, *7*, 4158–4176. [[CrossRef](#)]
20. Kim, N.-I.; Lee, C.-B.; Seo, J.-M.; Lee, W.-J.; Roh, Y.-B. Correlation between positive-electrode morphology and sulfur utilization in lithium-sulfur battery. *J. Power Sources* **2004**, *132*, 209–212. [[CrossRef](#)]
21. He, M.; Yuan, L.-X.; Zhang, W.-X.; Hu, X.-L.; Huang, Y.-H. Enhanced cyclability for sulfur cathode achieved by a water-soluble binder. *J. Phys. Chem. C* **2011**, *115*, 15703–15709. [[CrossRef](#)]
22. Rao, M.; Song, X.; Liao, H.; Cairns, E.J. Carbon nanofiber-sulfur composite cathode materials with different binders for secondary Li/S cells. *Electrochim. Acta* **2012**, *65*, 228–233. [[CrossRef](#)]

23. Rao, M.; Song, X.; Cairns, E.J. Nano-carbon/sulfur composite cathode materials with carbon nanofiber as electrical conductor for advanced secondary lithium/sulfur cells. *J. Power Sources* **2012**, *205*, 474–478. [[CrossRef](#)]
24. Hong, X.; Jin, J.; Wen, Z.; Zhang, S.; Wang, Q.; Shen, C.; Rui, K. On the dispersion of lithium-sulfur battery cathode materials effected by electrostatic and stereo-chemical factors of binders. *J. Power Sources* **2016**, *324*, 455–461. [[CrossRef](#)]
25. Lv, D.; Zheng, J.; Li, Q.; Xie, X.; Ferrara, S.; Nie, Z.; Mehdi, L.B.; Browning, N.D.; Zhang, J.-G.; Graff, G.L.; et al. High energy density lithium-sulfur batteries: Challenges of thick sulfur cathodes. *Adv. Energy Mater.* **2015**, *5*, 1402290. [[CrossRef](#)]
26. Lemarié, Q.; Alloin, F.; Thivel, P.X.; Idrissi, H.; Roué, L. Study of sulfur-based electrodes by operando acoustic emission. *Electrochim. Acta* **2019**, *299*, 415–422. [[CrossRef](#)]
27. Pang, Q.; Liang, X.; Kwok, C.Y.; Kulisch, J.; Nazar, L.F. A comprehensive approach toward stable lithium-sulfur batteries with high volumetric energy density. *Adv. Energy Mater.* **2016**, *7*, 1601630. [[CrossRef](#)]
28. Huang, X.; Luo, B.; Knibbe, R.; Hu, H.; Lyu, M.; Xiao, M.; Sun, D.; Wang, S.; Wang, L. An integrated strategy towards enhanced performance of the lithium-sulfur battery and its fading mechanism. *Chem. A Eur. J.* **2018**, *24*, 18544–18550. [[CrossRef](#)]
29. Waluś, S.; Robba, A.; Bouchet, R.; Barchasz, C.; Alloin, F. Influence of the binder and preparation process on the positive electrode electrochemical response and Li/S system performances. *Electrochim. Acta* **2016**, *210*, 492–501. [[CrossRef](#)]
30. Li, Y.; Zeng, Q.; Gentle, I.R.; Wang, D.-W. Carboxymethyl cellulose binders enable high-rate capability of sulfurized polyacrylonitrile cathodes for Li-S batteries. *J. Mater. Chem. A* **2017**, *5*, 5460–5465. [[CrossRef](#)]
31. Shaibani, M.; Mirshekarloo, M.S.; Singh, R.; Easton, C.D.; Cooray, M.C.D.; Eshraghi, N.; Abendroth, T.; Dörfler, S.; Althues, H.; Kaskel, S.; et al. Expansion-tolerant architectures for stable cycling of ultrahigh-loading sulfur cathodes in lithium-sulfur batteries. *Sci. Adv.* **2020**, *6*, eaay2757. [[CrossRef](#)] [[PubMed](#)]
32. Huang, Y.; Shaibani, M.; Gamot, T.D.; Wang, M.; Jovanovic, P.; Cooray, M.C.D.; Mirshekarloo, M.S.; Mulder, R.J.; Medhekar, N.V.; Hill, M.R.; et al. A saccharide-based binder for efficient polysulfide regulations in Li-S batteries. *Nat. Commun.* **2021**, *12*, 5375. [[CrossRef](#)] [[PubMed](#)]
33. Nara, H.; Yokoshima, T.; Mikuriya, H.; Tsuda, S.; Momma, T.; Osaka, T. The potential for the creation of a high areal capacity lithium-sulfur battery using a metal foam current collector. *J. Electrochem. Soc.* **2016**, *164*, A5026–A5030. [[CrossRef](#)]
34. Nakazawa, T.; Ikoma, A.; Kido, R.; Ueno, K.; Dokko, K.; Watanabe, M. Effects of compatibility of polymer binders with solvate ionic liquid electrolytes on discharge and charge reactions of lithium-sulfur batteries. *J. Power Sources* **2016**, *307*, 746–752. [[CrossRef](#)]
35. Liao, J.; Liu, Z.; Wang, J.; Ye, Z. Cost-effective water-soluble poly(vinyl alcohol) as a functional binder for high-sulfur-loading cathodes in lithium-sulfur batteries. *ACS Omega* **2020**, *5*, 8272–8282. [[CrossRef](#)] [[PubMed](#)]
36. Chen, F.; Li, H.; Chen, T.; Chen, Z.; Zhang, Y.; Fan, X.; Zhan, L.; Ma, L.; Zhou, X. Constructing crosslinked lithium polyacrylate/polyvinyl alcohol complex binder for high performance sulfur cathode in lithium-sulfur batteries. *Colloids Surf. A Physicochem.* **2021**, *611*, 125870. [[CrossRef](#)]
37. Zhang, Z.; Bao, W.; Lu, H.; Jia, M.; Xie, K.; Lai, Y.; Li, J. Water-soluble polyacrylic acid as a binder for sulfur cathode in lithium-sulfur battery. *ECS Electrochem. Lett.* **2012**, *1*, A34–A37. [[CrossRef](#)]
38. Pan, J.; Xu, G.; Ding, B.; Chang, Z.; Wang, A.; Dou, H.; Zhang, X. PAA/PEDOT:PSS as a multifunctional, water-soluble binder to improve the capacity and stability of lithium-sulfur batteries. *RSC Adv.* **2016**, *6*, 40650–40655. [[CrossRef](#)]
39. Fu, X.; Scudiero, L.; Zhong, W.-H. A robust and ion-conductive protein-based binder enabling strong polysulfide anchoring for high-energy lithium-sulfur batteries. *J. Mater. Chem. A* **2019**, *7*, 1835–1848. [[CrossRef](#)]
40. Yuan, Y.; Li, Z.; Lu, H.; Cheng, H.; Zheng, D.; Fang, Z. Investigation of a hybrid binder constitution for lithium-sulfur battery application. *New J. Chem.* **2020**, *44*, 10648–10653. [[CrossRef](#)]
41. Liu, Z.; He, X.; Fang, C.; Camacho-Forero, L.E.; Zhao, Y.; Fu, Y.; Feng, J.; Kostecky, R.; Balbuena, P.B.; Zhang, J.; et al. Reversible crosslinked polymer binder for recyclable lithium sulfur batteries with high performance. *Adv. Funct. Mater.* **2020**, *30*, 2003605. [[CrossRef](#)]
42. Xie, Z.H.; Huang, Z.X.; Rong, M.Z.; Zhang, M.Q. Imparting high robustness and suppression ability of shuttle effect to sulfur cathode in the Li-S battery via a novel multifunctional binder. *Mater. Today Energy* **2020**, *18*, 100555. [[CrossRef](#)]
43. Chuang, Y.-P.; Hong, J.-L. Triple cross-linked network derived from xanthan gum/sodium poly(acrylic acid)/metal ion as a functional binder of the sulfur cathode in lithium-sulfur batteries. *ACS Appl. Energy Mater.* **2021**, *4*, 10213–10221. [[CrossRef](#)]
44. Li, M.; Zhang, J.; Gao, Y.; Wang, X.; Zhang, Y.; Zhang, S. A water-soluble, adhesive and 3D cross-linked polyelectrolyte binder for high-performance lithium-sulfur batteries. *J. Mater. Chem. A* **2021**, *9*, 2375–2384. [[CrossRef](#)]
45. Wang, J.-T.; Chuang, Y.-P.; Wang, C.-C.; Hong, J.-L. Hydrogen bonds to balance mechanical and adhesive properties of pectin/polyacrylic acid blends as efficient binders for cathode in lithium-sulfur battery. *Mater. Today Commun.* **2022**, *31*, 103211. [[CrossRef](#)]
46. Hwa, Y.; Cairns, E.J. Polymeric binders for the sulfur electrode compatible with ionic liquid containing electrolytes. *Electrochim. Acta* **2018**, *271*, 103–109. [[CrossRef](#)]
47. Kim, H.M.; Hwang, J.Y.; Aurbach, D.; Sun, Y.K. Electrochemical properties of sulfurized-polyacrylonitrile cathode for lithium-sulfur batteries: Effect of polyacrylic acid binder and fluoroethylene carbonate additive. *J. Phys. Chem. Lett.* **2017**, *8*, 5331–5337. [[CrossRef](#)] [[PubMed](#)]

48. Cheon, S.-E.; Cho, J.-H.; Ko, K.-S.; Kwon, C.-W.; Chang, D.-R.; Kim, H.-T.; Kima, S.-W. Structural factors of sulfur cathodes with poly(ethylene oxide) binder for performance of rechargeable lithium sulfur batteries. *J. Electrochem. Soc.* **2002**, *149*, A1437–A1441. [[CrossRef](#)]
49. Liu, J.; Nara, H.; Yokoshima, T.; Momma, T.; Osaka, T. Li₂S cathode modified with polyvinylpyrrolidone and mechanical milling with carbon. *J. Power Sources* **2015**, *273*, 1136–1141. [[CrossRef](#)]
50. Lacey, M.J.; Osterlund, V.; Bergfelt, A.; Jeschull, F.; Bowden, T.; Brandell, D. A robust, water-based, functional binder framework for high-energy lithium-sulfur batteries. *ChemSusChem* **2017**, *10*, 2758–2766. [[CrossRef](#)]
51. Chien, Y.C.; Jang, H.; Brandell, D.; Lacey, M.J. Poly(ethylene glycol-block-2-ethyl-2-oxazoline) as cathode binder in lithium-sulfur batteries. *ChemistryOpen* **2021**, *10*, 960–965. [[CrossRef](#)] [[PubMed](#)]
52. Zhang, H.; Hu, X.; Zhang, Y.; Wang, S.; Xin, F.; Chen, X.; Yu, D. 3D-crosslinked tannic acid/poly(ethylene oxide) complex as a three-in-one multifunctional binder for high-sulfur-loading and high-stability cathodes in lithium-sulfur batteries. *Energy Storage Mater.* **2019**, *17*, 293–299. [[CrossRef](#)]
53. Do, V.; Lee, S.H.; Jang, E.; Lee, J.H.; Lee, J.W.; Lee, J.T.; Cho, W.I. Aqueous quaternary polymer binder enabling long-life lithium-sulfur batteries by multifunctional physicochemical properties. *ACS Appl. Mater. Interfaces* **2022**, *14*, 19353–19364. [[CrossRef](#)] [[PubMed](#)]
54. Wang, H.; Wang, Y.; Zhang, G.; Yang, Z.; Chen, Y.; Deng, Y.; Yang, Y.; Wang, C. Water-based dual-network conductive polymer binders for high-performance Li-S batteries. *Electrochim. Acta* **2021**, *371*, 137822. [[CrossRef](#)]
55. Zhang, L.; Ling, M.; Feng, J.; Liu, G.; Guo, J. Effective electrostatic confinement of polysulfides in lithium/sulfur batteries by a functional binder. *Nano Energy* **2017**, *40*, 559–565. [[CrossRef](#)]
56. Liao, J.; Liu, Z.; Liu, X.; Ye, Z. Water-soluble linear poly(ethylenimine) as a superior bifunctional binder for lithium-sulfur batteries of improved cell performance. *J. Phys. Chem. C* **2018**, *122*, 25917–25929. [[CrossRef](#)]
57. Akhtar, N.; Shao, H.; Ai, F.; Guan, Y.; Peng, Q.; Zhang, H.; Wang, W.; Wang, A.; Jiang, B.; Huang, Y. Gelatin-polyethylenimine composite as a functional binder for highly stable lithium-sulfur batteries. *Electrochim. Acta* **2018**, *282*, 758–766. [[CrossRef](#)]
58. Wang, H.; Ling, M.; Bai, Y.; Chen, S.; Yuan, Y.; Liu, G.; Wu, C.; Wu, F. Cationic polymer binder inhibit shuttle effects through electrostatic confinement in lithium sulfur batteries. *J. Mater. Chem. A* **2018**, *6*, 6959–6966. [[CrossRef](#)]
59. Gao, R.; Zhang, Q.; Zhao, Y.; Han, Z.; Sun, C.; Sheng, J.; Zhong, X.; Chen, B.; Li, C.; Ni, S.; et al. Regulating polysulfide redox kinetics on a self-healing electrode for high-performance flexible lithium-sulfur batteries. *Adv. Funct. Mater.* **2021**, *32*, 2110313. [[CrossRef](#)]
60. Liu, J.; Galpaya, D.G.D.; Yan, L.; Sun, M.; Lin, Z.; Yan, C.; Liang, C.; Zhang, S. Exploiting a robust biopolymer network binder for an ultrahigh-areal-capacity Li-S battery. *Energy Environ. Sci.* **2017**, *10*, 750–755. [[CrossRef](#)]
61. Liu, J.; Sun, M.; Zhang, Q.; Dong, F.; Kaghazchi, P.; Fang, Y.; Zhang, S.; Lin, Z. A robust network binder with dual functions of Cu²⁺ ions as ionic crosslinking and chemical binding agents for highly stable Li-S batteries. *J. Mater. Chem. A* **2018**, *6*, 7382–7388. [[CrossRef](#)]
62. Liu, X.; Qian, T.; Liu, J.; Tian, J.; Zhang, L.; Yan, C. Greatly improved conductivity of double-chain polymer network binder for high sulfur loading lithium-sulfur batteries with a low electrolyte/sulfur ratio. *Small* **2018**, *14*, 1801536. [[CrossRef](#)] [[PubMed](#)]
63. Jin, B.; Yang, L.; Zhang, J.; Cai, Y.; Zhu, J.; Lu, J.; Hou, Y.; He, Q.; Xing, H.; Zhan, X.; et al. Bioinspired binders actively controlling ion migration and accommodating volume change in high sulfur loading lithium-sulfur batteries. *Adv. Energy Mater.* **2019**, *9*, 1902938. [[CrossRef](#)]
64. Chu, Y.; Chen, N.; Cui, X.; Liu, A.; Zhen, L.; Pan, Q. A multi-functional binder for high loading sulfur cathode. *J. Energy Chem.* **2020**, *46*, 99–104. [[CrossRef](#)]
65. Rashid, A.; Zhu, X.; Wang, G.; Ke, C.; Li, S.; Sun, P.; Hu, Z.; Zhang, Q.; Zhang, L. Highly integrated sulfur cathodes with strong sulfur/high-strength binder interactions enabling durable high-loading lithium-sulfur batteries. *J. Energy Chem.* **2020**, *49*, 71–79. [[CrossRef](#)]

Disclaimer/Publisher’s Note: The statements, opinions and data contained in all publications are solely those of the individual author(s) and contributor(s) and not of MDPI and/or the editor(s). MDPI and/or the editor(s) disclaim responsibility for any injury to people or property resulting from any ideas, methods, instructions or products referred to in the content.